

THE EVAPORATION AND BURNING OF LIQUID FUEL DROPS

Jay A. Bolt  
Thomas A. Boyle  
William Mirsky  
University of Michigan

Engineering Research Institute Project No. 1988-6-F  
Power Plant Laboratory  
Contract No. AF33(600)-5057  
Task No. 30236

Wright Air Development Center  
Air Research and Development Command  
United States Air Force  
Wright-Patterson Air Force Base, Ohio

enqn  
UMR 443

#### FOREWORD

This report was prepared by the Engineering Research Institute of the University of Michigan under USAF Contract AF 33(600)-5057, Supplemental Agreement No. S2(53-308). The contract was initiated under research and development project identified by Expenditure Order No. R-533-106C "Fuel Nozzles," and completed under Task No. 30236, "Fuel Nozzle Program." It was administered under the direction of the Power Plant Laboratory, Wright Air Development Center, with Mr. J. W. Fulton, acting as project coordinator.

## ABSTRACT

This report is concerned with the evaporation and combustion of liquid fuel drops in the range of sizes used in aircraft gas turbine combustors.

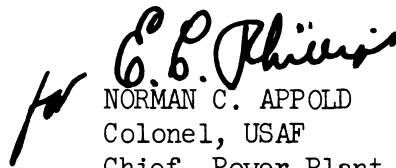
Clouds of uniform size fuel drops in the size range of 70 to 150 microns diameter were produced by means of a spinning disc. A photographic technique was used to obtain an indication of the rate of change of diameter and the velocity of the burning drops, while moving freely in air. The mass rate of burning was found to be proportional to the first power of the drop diameter.

Equipment has been developed which permits a drop to be stabilized in space by means of air drag forces and an ultrasonic field. Data on drop evaporation taken with this equipment reveals that for drops of initial size of 800 to 1300 microns a linear relationship exists between droplet diameter and elapsed time of evaporation. It has been determined that the ultrasonic field increases the rate of evaporation, the rate increasing with increased field intensity.

## PUBLICATION REVIEW

The publication of this report does not constitute approval by the Air Force of the findings or the conclusions contained herein. It is published only for the exchange and stimulation of ideas.

FOR THE COMMANDER:

  
NORMAN C. APPOLD  
Colonel, USAF  
Chief, Power Plant Laboratory

## TABLE OF CONTENTS

	Page
FOREWORD	ii
ABSTRACT	iii
LIST OF TABLES	v
LIST OF FIGURES	vi
SUMMARY OF PREVIOUS WORK	1
SUMMARY OF PREVIOUS WORK DONE UNDER THIS CONTRACT	1
SECTION I: COMBUSTION OF GROUPS OF DROPS	11
Experimental Work	11
SECTION II: EVAPORATION OF INDIVIDUAL DROPS	13
Introduction	13
Description of Apparatus	13
The Barium Titanate Piezoelectric Transducer	19
Experimental Procedure	23
Experimental Results	28
Effect of the Ultrasonic Field on Evaporation	31
BIBLIOGRAPHY	33
APPENDIX A: BURNING DROPS - DATA SUMMARY FOR FOUR HYDROCARBON FUELS	35
APPENDIX B: DEVELOPMENT OF THE EQUATION FOR THE STABILIZING ACTION OF THE ULTRASONIC FIELD ON DROP POSITION	42
APPENDIX C: TEMPERATURES AT WHICH A STATIONARY SOUND FIELD IS ESTABLISHED IN THE PIEZOELECTRIC TUBE	47

## LIST OF TABLES

Table No.	Title	Page
I	Rate of Combustion of Four Hydrocarbons	11
II	Combustion Data from Photographs with Vertical Plane	12
III	Evaporation Rates of Some Hydrocarbon Fuels	32

## LIST OF FIGURES

Figure No.	Title	Page
1	Equipment for Making, Burning, and Photographing Uniform Size Fuel-Drops	2
2	Photograph of Drop Combustion Equipment	3
3	Photograph of Drop Combustion Equipment, Showing Kerosene Spray Burning in Heated Air	3
4	Photograph Showing Double Images of Burning Kerosene Drops in Combustion Zone - Initial Drop Diameter - 100 Microns	4
5	Mean Diameter Squared vs Elapsed Time 80 Micron Benzene Drops	5
6	Mean Diameter Squared vs Elapsed Time 100 Micron n-Heptane Drops	6
7	Mean Diameter Squared vs Elapsed Time, 80 Micron Propanol Drops	7
8	Mean Diameter Squared vs Elapsed Time 100 Micron Cyclohexane Drops	8
9	Photograph of Burning Drops with Axis of Camera Horizontal	9
10	Photograph of Burning Drops with Axis of Camera Horizontal (Plane of Picture Vertical) - Heated Air Supply	10
11	Schematic of Equipment Set-Up, Single Droplet Technique	14
12	Photograph of Equipment Set-Up, Single Droplet Technique	14
13	Nozzle Contour - Archimedes Spiral	15
14	Schematic of Ultrasonic Frequency Amplifier	15
15	Cut-Away View of Lens Extension Tube	16
16	Close-Up View of Camera, Barium Titanate Tube, and Droplet Light	18
17	Schematic of Switch Box	18
18	Basic Piezoelectric Elements	20
19	Action of the Piezoelectric Tube Under Changes in Polarity of Applied Voltage	20
20	Generation of the Standing Sound Wave by the Piezoelectric Tube	22
21	Section of 16-mm Film Showing Change from Stop-Watch to Droplet Image	22
22	Sequence of Frames Taken from a Film of an Evaporating Droplet (Acetophenone)-Elapsed Time Given in Minutes and Seconds	24

## LIST OF FIGURES (Cont.)

Figure No.	Title	Page
23	Evaporation Curves for Some Pure Hydrocarbons, Diameter vs Elapsed Time	25
24	Evaporation Curves for Some Pure Hydrocarbons, Diameter vs Elapsed Time	26
25	Evaporation Curves, Diameter vs Elapsed Time	27
26	Boiling Point and Latent Heat of Vaporization as a Function of Evaporation Rate for Some Pure Hydrocarbons	29
27	Effect of Ultrasonic Field Intensity on Evaporation Rates (Tert-Butylbenzene)	30

## SUMMARY OF PREVIOUS WORK

In an effort to learn about the combustion of fuel drops of approximately 100 microns diameter three somewhat interdependent schemes have been pursued:

1. Burn single drops of 1000-2000 microns or larger original diameter and extrapolate the results into the region of interest. In practically all of the work of this type the drops have been suspended on a filament or represented by porous spheres wetted with the fuel under study (Godsave<sup>2</sup> and Spalding<sup>6</sup>). The method has several distinct advantages: The location of the drop is fixed and the drop is easily photographed. With sufficiently large initial diameter acceptable accuracy may be had either by photographing the suspended drop or measuring the fuel flowing to the porous quasi drop.

In contrast to the advantages, the method introduces the possibility of complication arising from the presence of the filament used to support the drop; this also serves to limit the minimum diameters.

Moreover, the possibility exists that, although regularities are observed in the evaporation and combustion of drops 1000 microns and larger, these regularities are not reliable for purposes of extrapolation into the range of size of interest. The results of these experiments are also difficult to adapt to groups of drops.

2. A second method is, of course, to build acceptable theory to account for the behavior of the drops. Such theory will be implemented by experimentally determined property values, or by assumptions, in some cases based upon photographic studies carried out as above. The paucity of basic data is such that one usually finds many assumptions are necessary.
3. A third possible approach to studying the combustion of drops of the order of 100 microns original diameter is to apply established means of photographic spray analysis - to a sample of the spray as it proceeds to evaporate and burn. This is the general line of procedure followed in the work covered in this section of the report.

## SUMMARY OF PREVIOUS WORK DONE UNDER THIS CONTRACT

Previous work carried out under this contract dealt with the producing, burning, and observing of groups of uniform size drops of 100-120 microns initial diameter. The work reported herein augments that reported previously in Reference (1). A brief resume of this work follows:

The spinning disk sprayer was used as the drop source because it was determined that this device would yield spray from 60 to 140 microns diameter with acceptable uniformity. Acceptable uniformity was arbitrarily taken to be represented by a spray with standard mean deviation of 5 microns. The limits of sprayer operation satisfying the requirements of uniformity were determined by examining the spray by means of photographs.

The spray delivered by the disk was burned in the form of a concentric ring about the disk, in a horizontal plane. The analysis of the burning spray was based upon a series of photographs taken vertically downward through the flame. See figures 1, 2, and 3, which are reproduced from Reference (1). These photographs revealed the successive reduction of diameter as the drops passed through the flame. They also revealed that the uniformity of size and velocity of the spray in the flame zone was considerably diminished as burning proceeds.



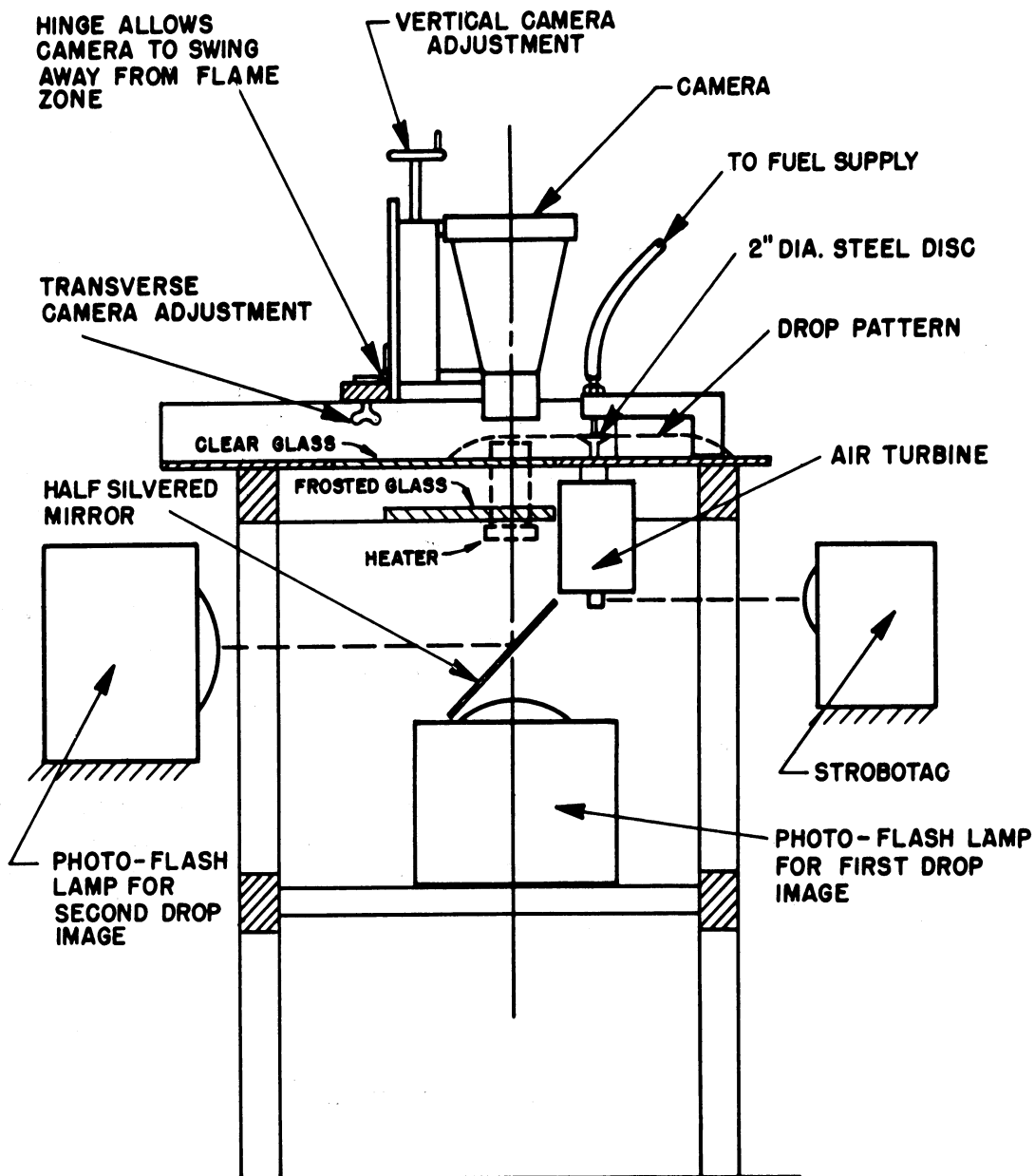


Fig. 1. Equipment for Making, Burning, and Photographing Uniform Size Fuel-Drops.

By taking a series of double flash pictures the velocity and diameter of a number of drops were determined, see Figure 4. Combining and averaging the results of a number of these photographs yielded the average time necessary for burning a fuel drop from 100 to 120 microns diameter, to 50 or 60 microns diameter. The time for combustion of the entire drop was determined by extrapolating to zero diameter. The time thus determined for the evaporation and combustion of a 100 micron drop of kerosene varied from 0.01 to 0.0267 second, for the conditions of the test.

For one series of photographs air was supplied through a tubular air heater. This procedure aided in burning somewhat larger drops (120-130 microns). Similar analysis of these photographs did not reveal any significant change in burning time.

Practically all initial work was done using kerosene as the fuel. Some trials had been made with single component fuels; the continuation of this work is reported below.

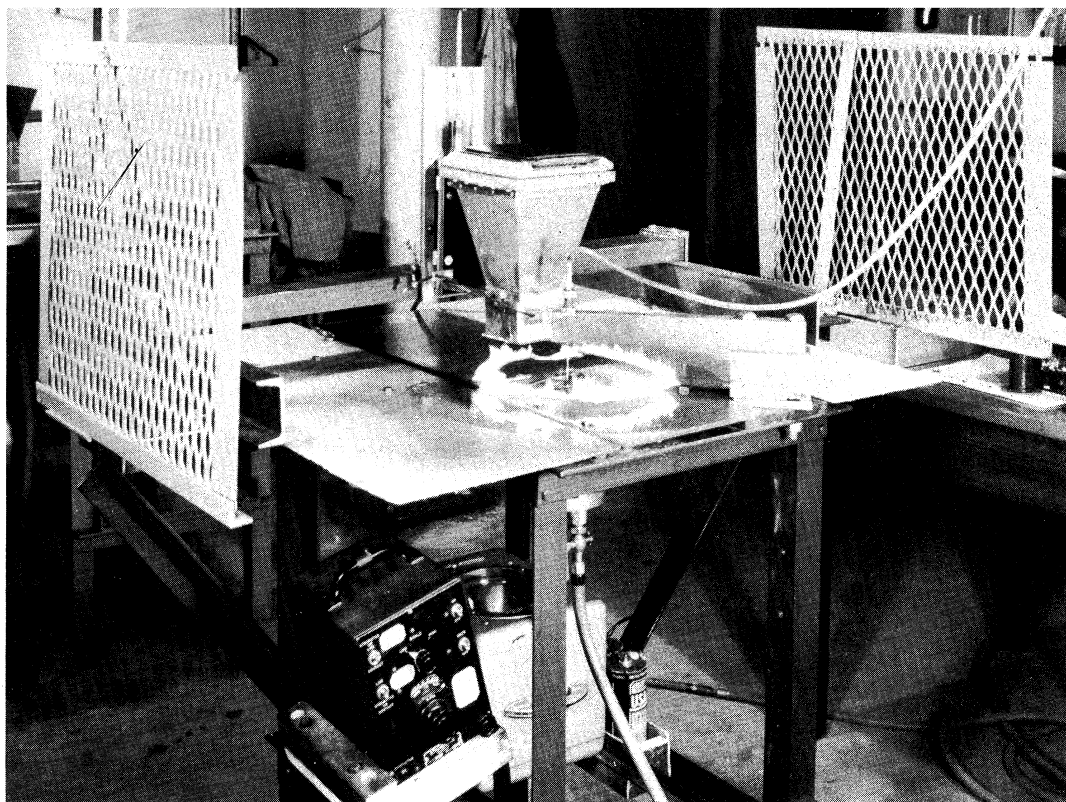


Fig. 2. Photograph of Drop Combustion Equipment.

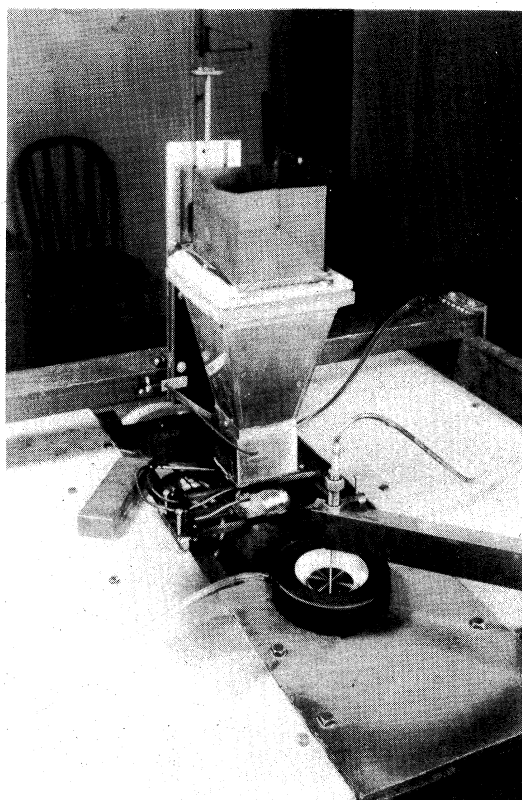


Fig. 3. Photograph of Drop Combustion Equipment, Showing Kerosene Spray Burning in Heated Air.



Fig. 4. Photograph Showing Double Images of Burning Kerosene Drops in Combustion Zone - Initial Drop Diameter - 100 Microns. •

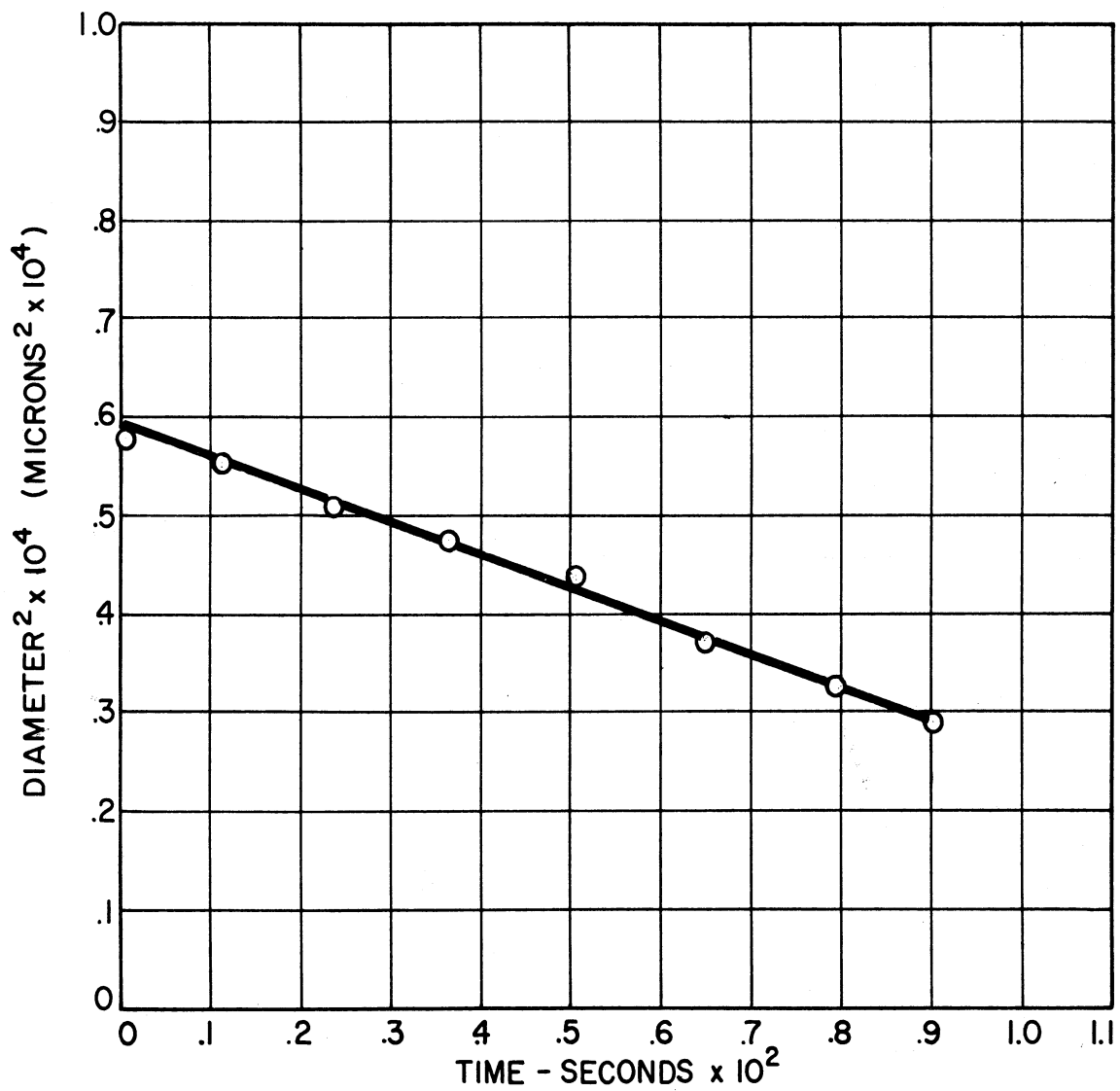


Fig. 5. Mean Diameter Squared vs Elapsed Time 80 Micron Benzene Drops.

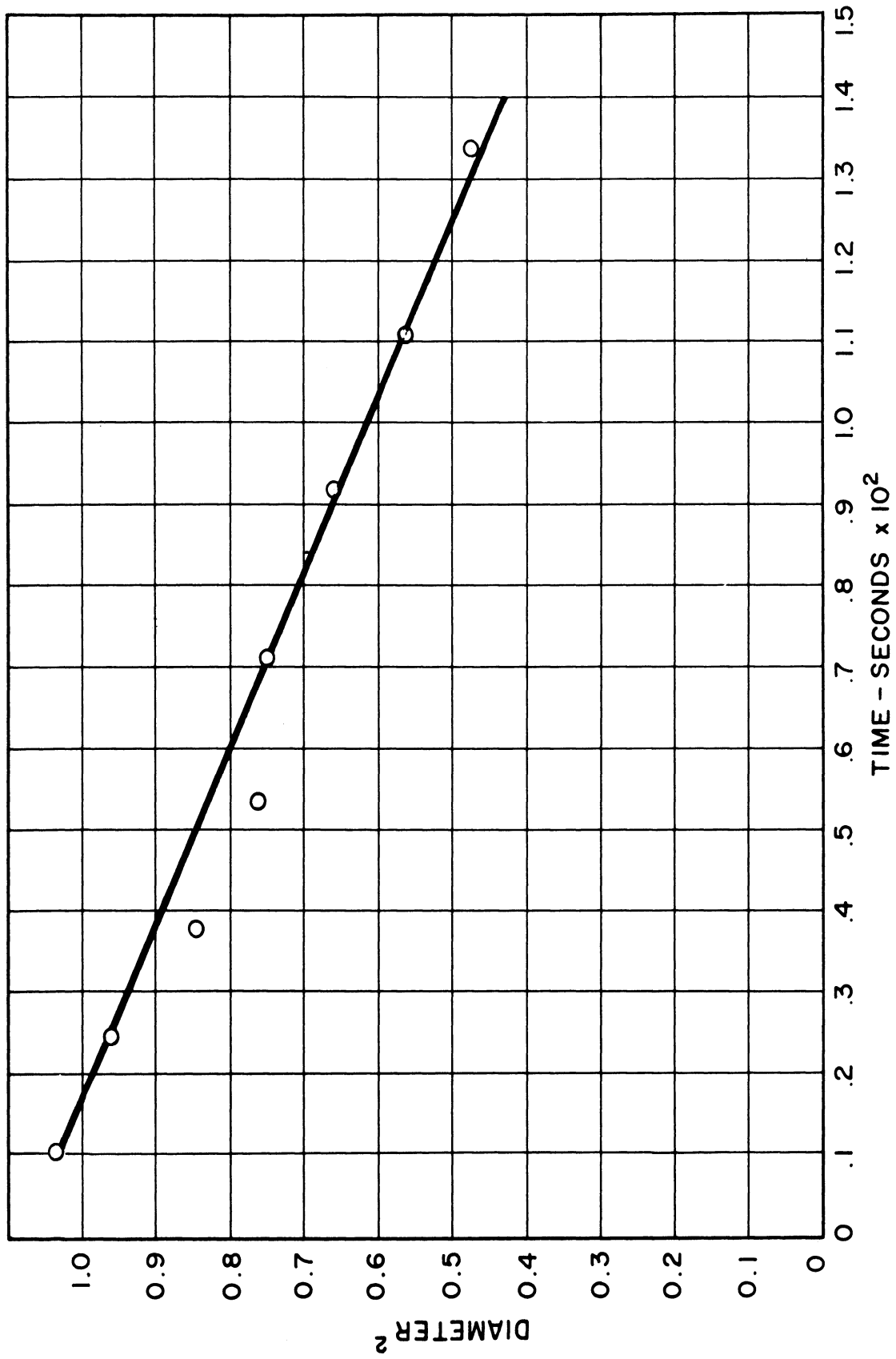


Fig. 6. Mean Diameter Squared vs Elapsed Time 100 Micron n-Heptane Drops.

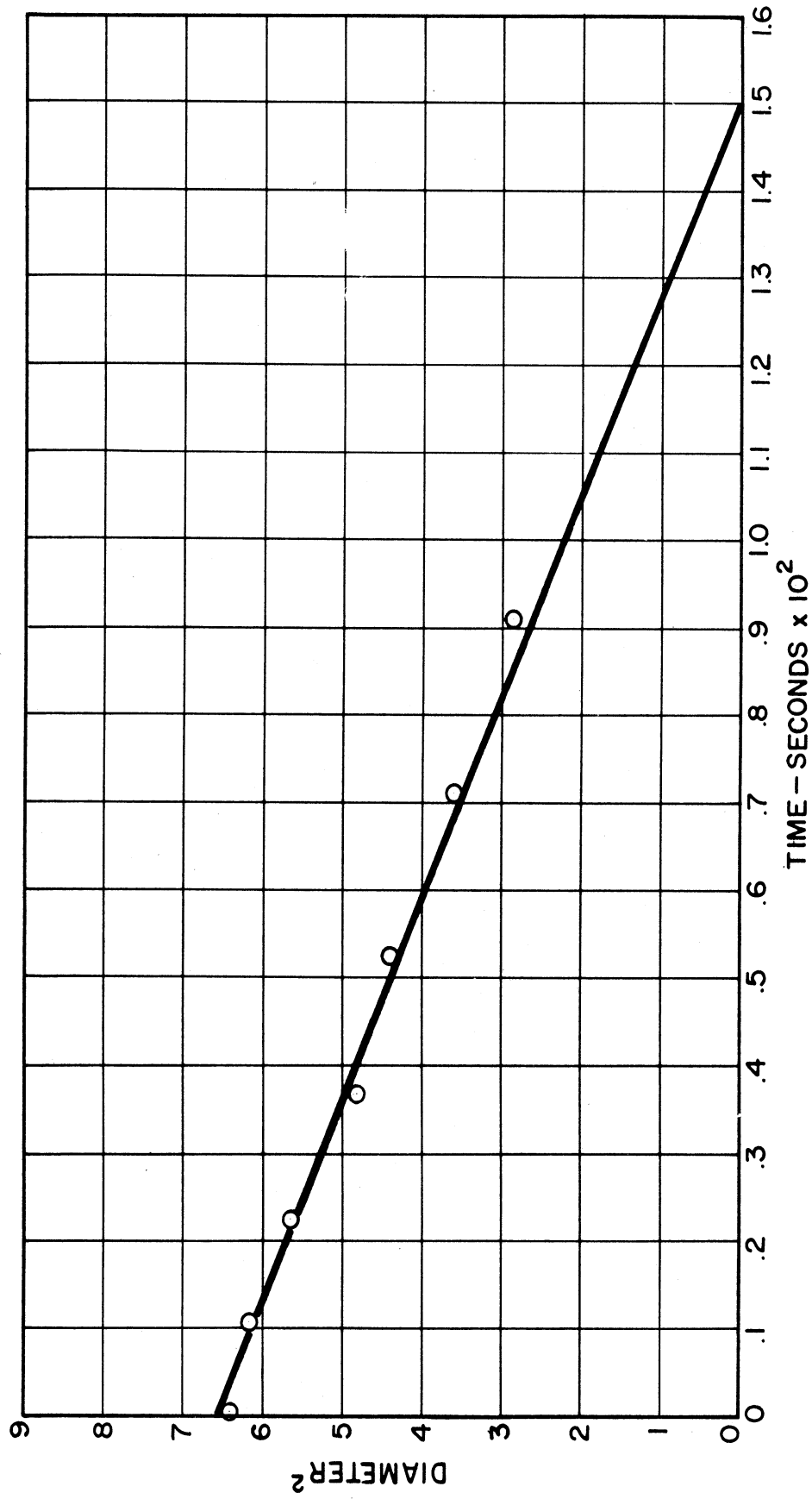


Fig. 7. Mean Diameter Squared vs Elapsed Time, 80 Micron Propanol Drops.

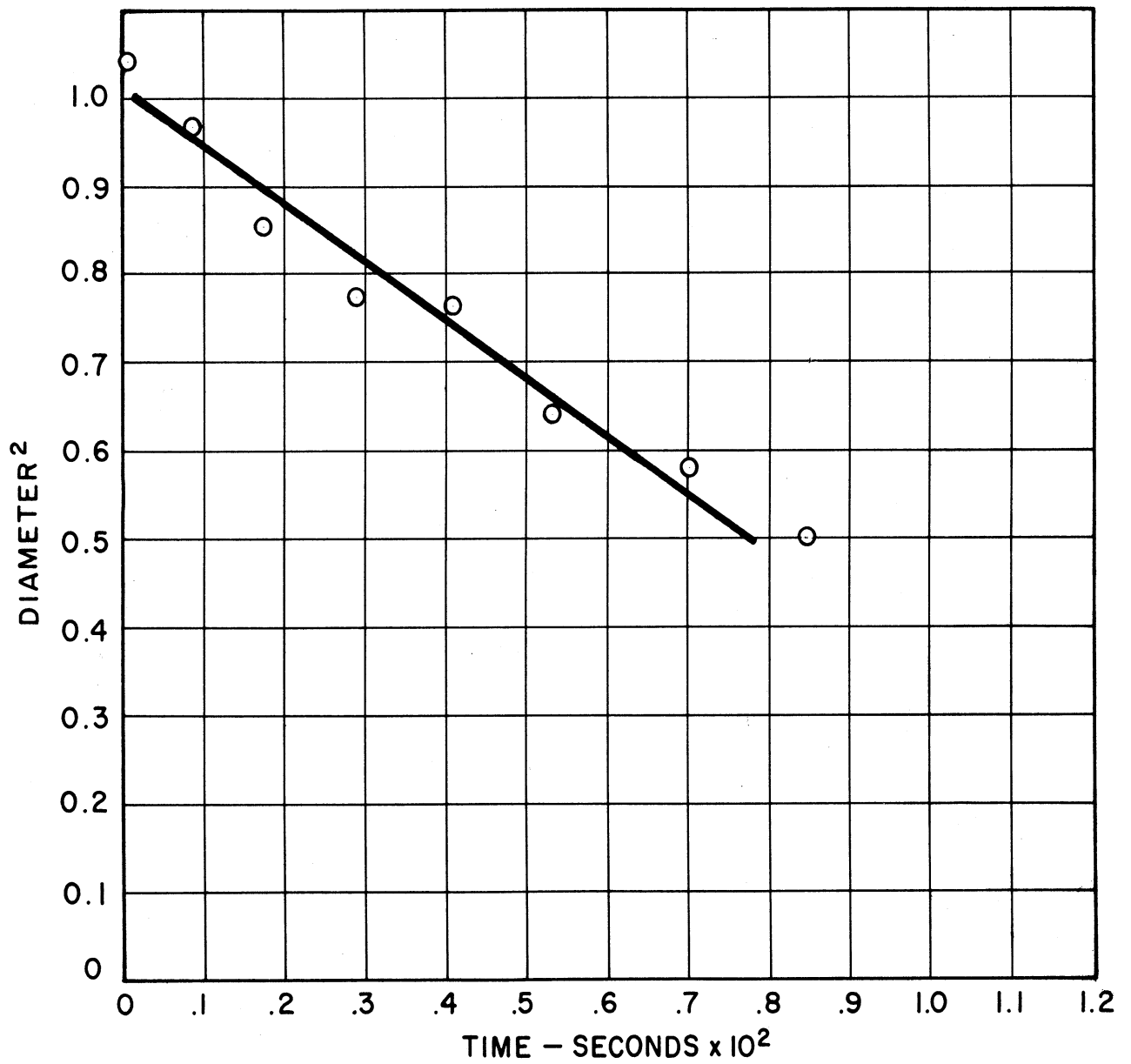


Fig. 8. Mean Diameter Squared vs Elapsed Time 100 Micron Cyclohexane Drops.



Fig. 9. Photograph of Burning Drops with Axis of Camera Horizontal.





Fig. 10. Photograph of Burning Drops with Axis of Camera Horizontal  
(Plane of Picture Vertical) - Heated Air Supply.

## SECTION I

### COMBUSTION OF GROUPS OF DROPS

#### Experimental Work

A detailed analysis was made for burning sprays of benzene, cyclohexane, n-propyl alcohol, and n-heptane. The photographic negatives were examined on a comparator with a total magnification of 30. The negatives were divided into zones, and the zones were aligned as described in detail in Reference (1). Summaries of the resulting drop counts will be found in Appendix A.

The data for this work was taken from 29 photographs, this number representing the productive group of some 250 photographs taken. The data is plotted showing the square of the mean drop diameter versus the elapsed time. As can be seen in Figures 5, 6, 7, and 8, the resulting plot closely follows a straight line down to a size of about 50 microns. The slope of this line is the constant  $\lambda$  for the particular fuel, as defined below. Given the value of  $\lambda$  for a particular fuel the time for evaporation and burning can be obtained readily from

$$D^2 = D_0^2 - \lambda t$$

where

D = diameter at time t

$D_0$  = original diameter

t = elapsed time, seconds

$\lambda$  = evaporation constant,  $\text{cm}^2/\text{sec}$

Results for the four fuels tested are presented by means of the values of  $\lambda$  taken from the plot as well as showing the corresponding life of a drop of 100 microns original diameter.

The data for these burning tests are shown in Appendix A for these four fuels; the most significant items of interest are shown in Table I, which follows:

TABLE I

Rate of Combustion of Four Hydrocarbons

Fuel	$\lambda(\text{cm}^2/\text{sec})$	Time to Evaporate 100 $\mu$ drop - seconds
Benzene	.0033	.03
Cyclohexane	.0066	.015
n-Propyl alcohol	.0046	.0217
n-Heptane	.0047	.0213

In pursuing this method some question arose as to whether a significant proportion of the smaller drops drifted up with convection currents within the flame zone. The photographs serving as the basis for the foregoing work were taken with the axis of the camera vertical, the region of focus being about 0.6 mm in depth and located close to the bottom of the flame. Any drift of small drops up out of the zone of focus of the camera would result in an apparent increase of the mean drop diameter remaining in focus in each succeeding zone, and therefore a deceptively low value of  $\lambda$  with a correspondingly long drop life.

To check this a series of photographs were taken at right angles to those mentioned above. The drops coming from part of the spinning disk were shielded and the camera was located in the shielded space with its axis tangential to the group

of drops that was burning. When viewed thus the flame presented a roughly triangular outline and revealed the drop images concentrated along the lower boundary of the flame (see Figure 9). It was noted that when heated air was supplied from below, through the tubular air heater, some small drops were observed rising through the flame zone, certainly out of focus of the vertically oriented camera (see Figure 10). The proportion of drops rising in flames without heated air supply appeared much lower.

A series of these photographs were analyzed for purposes of checking the values presented above. It should be pointed out that the numbers of drops appearing in focus are much smaller, therefore the resulting values would be more sensitive to anomalies and correspondingly less reliable. They are presented for two of the fuels in Table II.

TABLE II  
Combustion Data from Photographs with Vertical Plane

Fuel	$\lambda$	Time to evaporate 100 $\mu$ drop-seconds
Cyclohexane	.00763	.013
n-Heptane	.0091	.011

The results from the two methods are seen to agree in one instance, yet differ by roughly a factor of two in another. This irregularity may be attributed to the limited number of drops dealt with in one method, or to the apparent drop life being artificially lengthened by virtue of the small drops going out of focus in the other.

In order to compare the burning times of different fuel drops it would be desirable that the individual burning times be measured more accurately. The burning times reported here may be artificially long because of the dearth of small size drops.

Work has been done in an effort to improve the accuracy of the measurements of the rate of burning of the drops. One method consists of having a series of six flashes from a single flash lamp, during the life of the drops. In this manner a complete history can be obtained for a particular drop. This has been accomplished, and work is being done to improve this technique.

## SECTION II

### EVAPORATION OF INDIVIDUAL DROPS

#### Introduction

This investigation was originated to study the burning process of single droplets of various fuels. A subsequent evaporation study was initiated with the intention of adapting the techniques developed in the evaporation study to the study of the single droplet combustion process. Preliminary work led to the development of a technique whereby single droplets of fuel could be maintained in a fixed position by means of a vertical blast of air passing through a stationary ultrasonic field. This is the technique being used at the present time to study the evaporation of droplets. At the same time, the apparatus is being further developed to adapt the technique to the combustion study of single droplets. The original apparatus and technique have been described elsewhere<sup>(1)</sup>

This report describes the apparatus as modified since the appearance of the original report. Changes which are being considered in the hope of increasing the versatility and scope of operation of this technique are also described. All results obtained up to the writing of this report are included, but a full evaluation of these results has been delayed because of the undetermined effect of the stationary ultrasonic field on the evaporation process. Inconclusive tests relating to the ultrasonic effects are described briefly, and their preliminary results are given.

#### Description of Apparatus

Principal components of the apparatus used for freely suspending droplets are shown schematically in Fig. 11, while an actual view is given in Figure 12. These components include a surge tank, wind tunnel and nozzle, barium titanate piezoelectric tube, oscillator, amplifier, and camera.

A hot water tank, rated at 150 psig continuous duty, serves as the surge tank. No modifications were required to adapt the unit to the system since normal working pressure during operation of the apparatus is about 95 psia.

The vertical wind tunnel is composed of three sections: diffuser, calming section, and nozzle. Both the diffuser and calming sections are constructed from one-half inch white pine boards, fastened together with cross members as seen in Figure 12. Overall dimensions of the diffuser section are 21 x 21 x 31 inches high, the divergent angle being 30 degrees. The calming section is 21 x 21 x 19 inches high and contains a series of screens as indicated in Figure 11. Screen mesh starts at 20 x 20 at the lower part and increases in jumps of 20 x 20 up to 100 x 100, each screen being placed two inches above the next lower screen. The function of these screens is to progressively decrease the turbulence existing in the air flow before the air enters the nozzle.

The nozzle at the top of the wind tunnel is cut from a large block made up of 1-1/2 x 6 inch boards glued and then bolted together with four through bolts, the dimensions of the finished block being 21 x 21 x 6 inches high. The bolts are located so as not to interfere with the contour cutting operation described below. Cutting was done with a large flycutter, in the form of the Archimedes spiral shown in Figure 13, mounted in a vertical drill press. Considerable chatter developed as the cutting progressed, but this was eliminated each time by changing the speed of the drill press. Small cracks were then filled in with body putty and the nozzle sanded and varnished. A one-half inch aluminum plate with a 1-5/8 inch

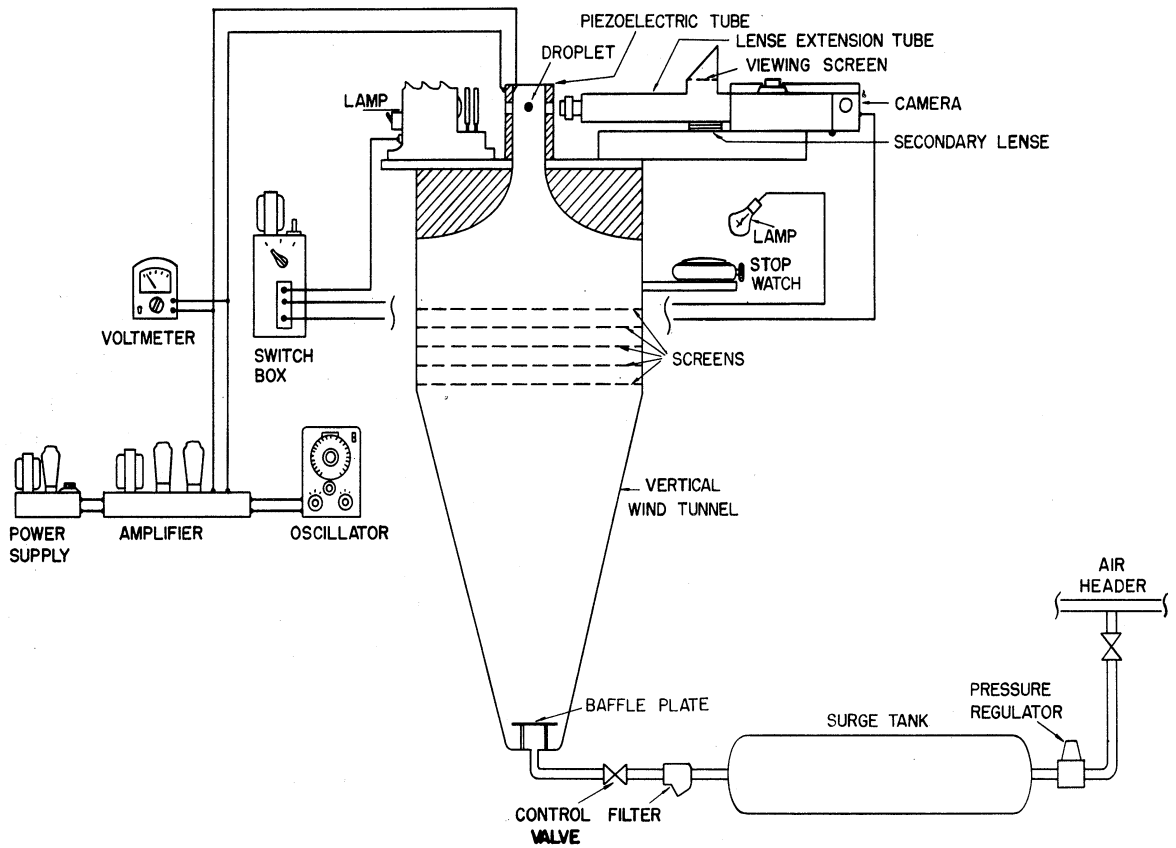


Fig. 11. Schematic of Equipment Set-Up, Single Droplet Technique.

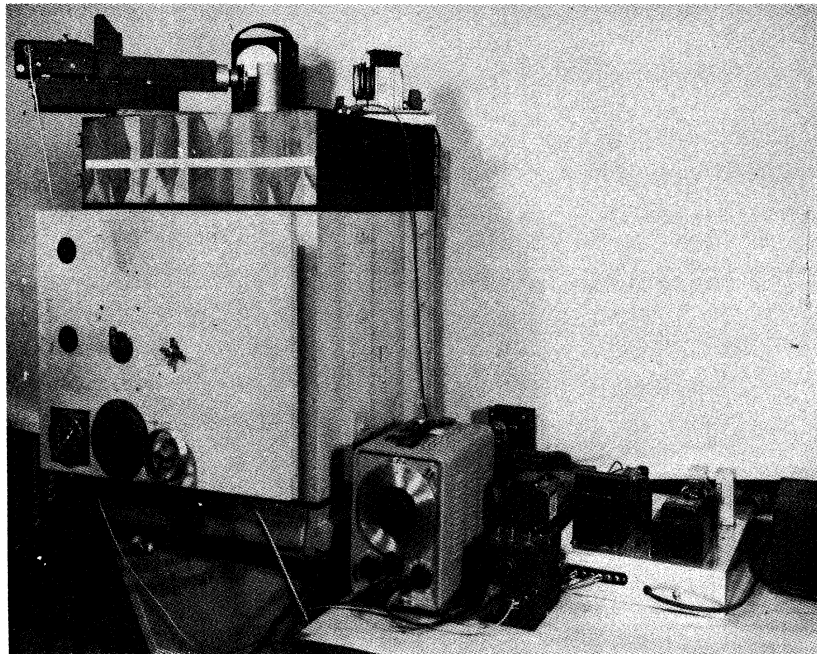


Fig. 12. Photograph of Equipment Set-Up, Single Droplet Technique.

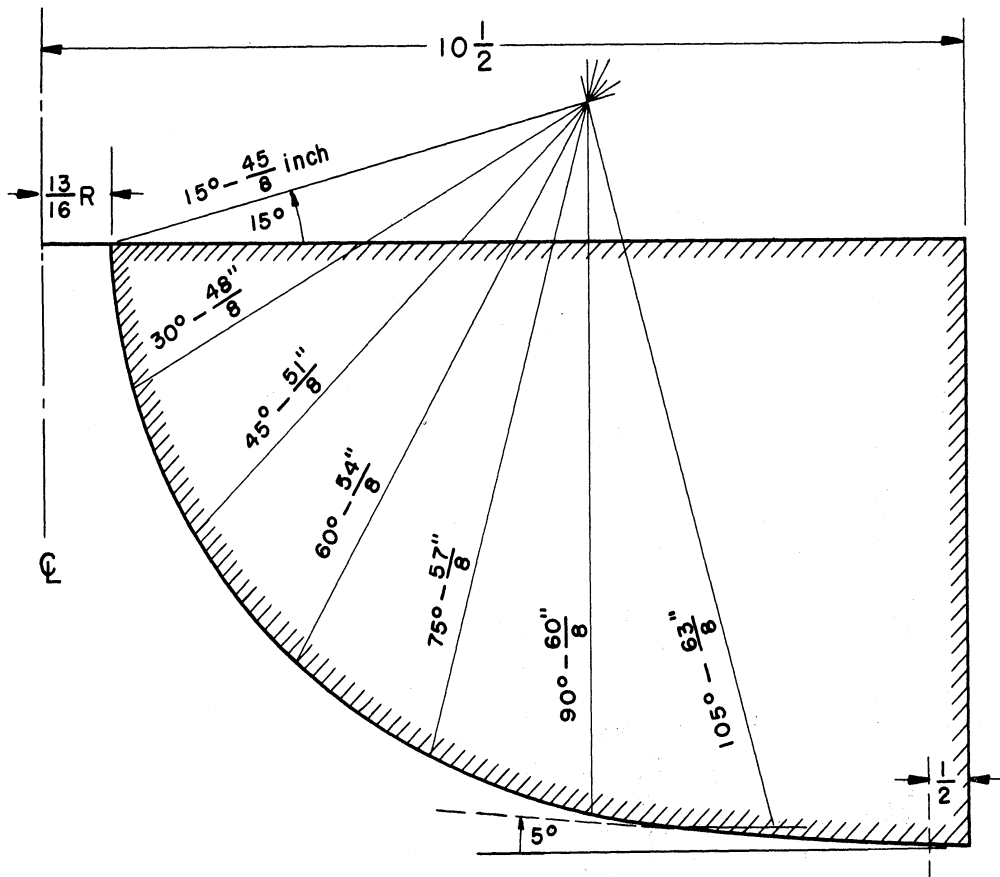
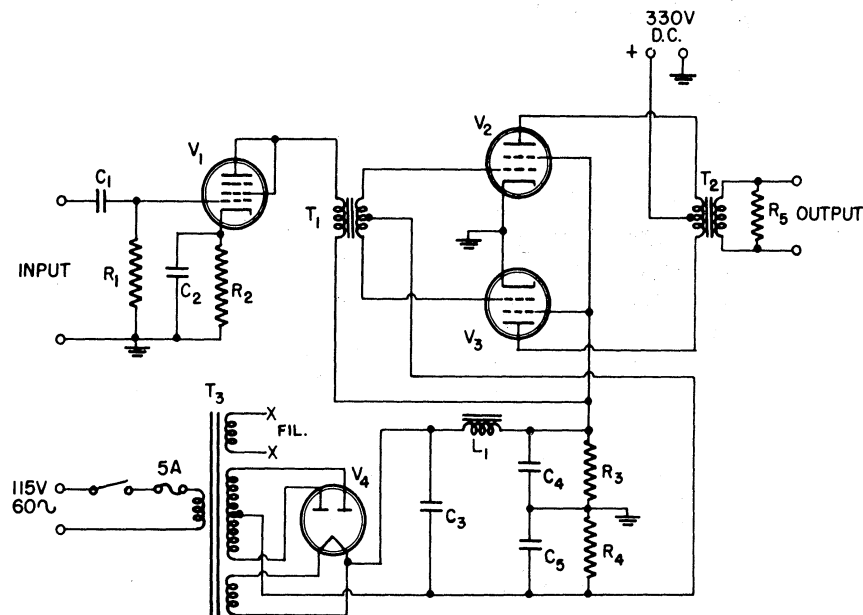


Fig. 13. Nozzle Contour - Archimedes Spiral.



$V_1 = 6F6$   
 $V_2, V_3 = 6L6$   
 $V_4 = 5U4G$   
 $R_1 = 0.5 \text{ MEG.}, 1/2 \text{ W}$   
 $R_2 = 1700, 1/2 \text{ W}$   
 $R_3 = 5.1\text{K}, 30 \text{ W}$   
 $R_4 = 200, 10 \text{ W}$   
 $R_5 = 2250, 25 \text{ W}$

$C_1 = 10 \text{ mfd.}, \text{ MICA}$   
 $C_2, C_5 = 25 \text{ mfd.}, 25 \text{ V.}$   
 $C_3, C_4 = 4 \text{ mfd.}, 400 \text{ V.}$   
 $L_1 = 4 \text{ H AT } 130 \text{ ma.}, 100 \text{ Ohms}$

$T_3 = \text{POWER TRANSFORMER}$   
 $375 - 375 \text{ VOLTS AT}$   
 $150 \text{ ma. D.C.}$

$T_1 = \text{DRIVER TRANSFORMER,}$   
 $\text{TURNS RATIO, PRI - } 1/2 \text{ SEC.} = 4:1$   
 $T_2 = \text{OUTPUT TRANSFORMER}$   
 $3800 \text{ OHM PRIMARY TO}$   
 $500 \text{ OHM SECONDARY}$

Fig. 14. Schematic of Ultrasonic Frequency Amplifier.

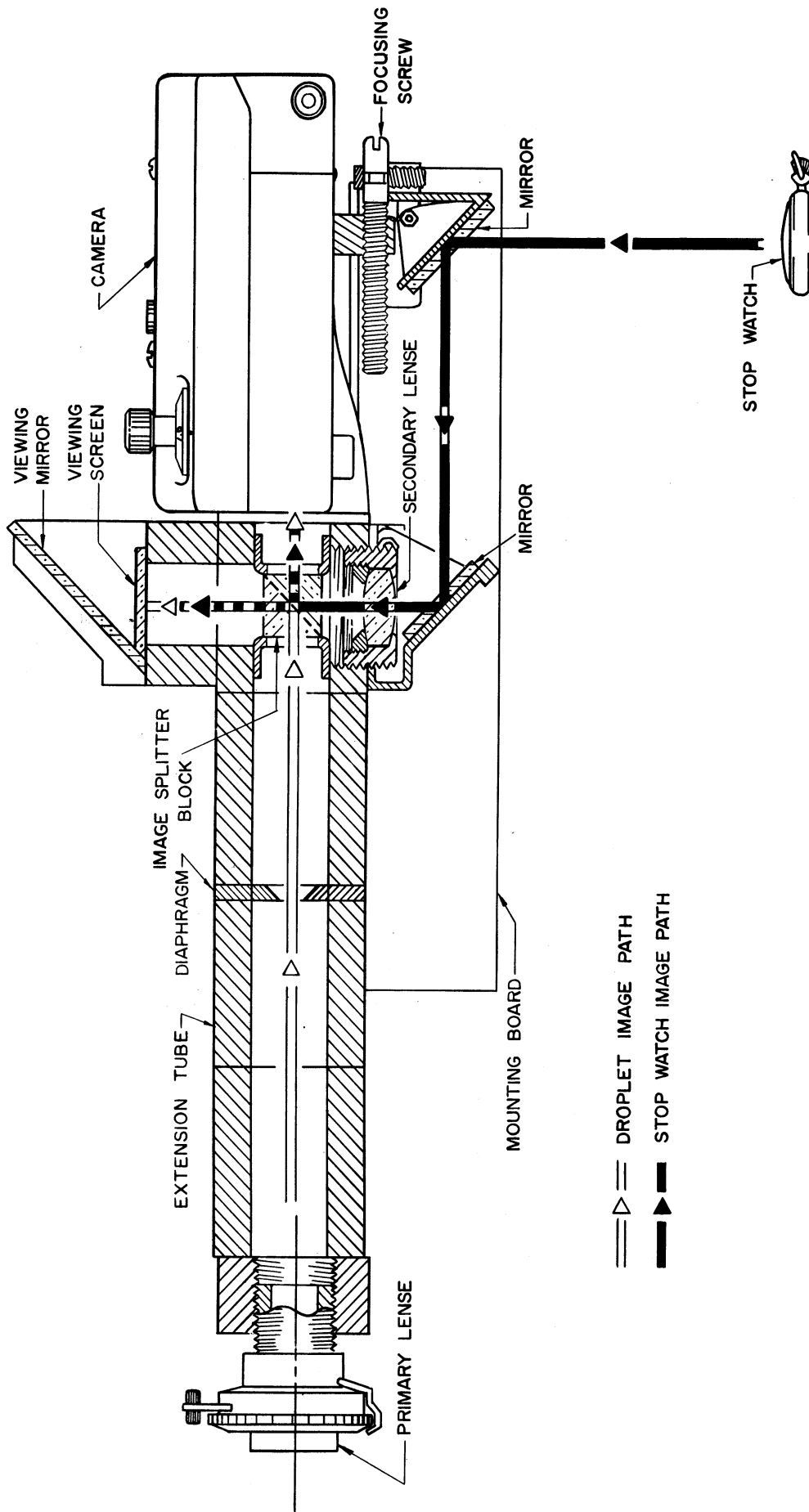


Fig. 15. Cut-Away View of Lens Extension Tube

hole in the center was bolted over the nozzle exit and serves as the mounting plate for the barium titanate tube.

Generation of the stationary ultrasonic field by the barium titanate tube is by the piezoelectric effect. The tube, after installation of the windows and tuning as described in a later section, mounts directly into the aluminum plate and makes electrical contact at both the inner and outer surfaces with spring contactors, electrically insulated from the aluminum plate. The contactors connect directly to the output of the ultrasonic frequency amplifier which in turn obtains its signal from the variable frequency oscillator. A schematic diagram of the amplifier is given in Figure 14.

Records of the evaporation runs were taken with a 16 mm U. S. Army Air Force Type N-6 gun camera having speeds of 16, 32, and 64 frames per second. To increase the drop image sharpness, the projection box used in the original set-up was replaced by a lens extension tube. The tube, made of one-half inch micarta, has an overall length of 11-1/4 inches, giving a magnification of 5X when used with a 50 mm focal length lens. The particular lens being used is a 50 mm, f/4.5 Wollensak Raptar in a Rapax shutter. The inside of the extension tube is lined with black velvet, and a black paper diaphragm is inserted in the tube to cut down light reflections from the tube wall. An image splitting block is mounted in the center of the tube at the camera end as shown in the cut-away view in Figure 15. The ground glass viewing screen and secondary lens are located directly above and below the block respectively. The focal length of the secondary lens was chosen so that the image of the stop watch just filled the frame of the 16 mm film.

The image splitting block divides the images from both lenses; the transmitted image passes directly through the block, the reflected image is reflected at 90 degrees. The transmitted drop image from the primary lens appears on the film while the reflected drop image appears on the viewing screen. The reverse is true for the stop watch image projected by the secondary lens. Using this arrangement, it is possible to view the droplet for position control purposes as it is being photographed. Figure 16 gives a close-up of the camera and piezoelectric tube in position on the wind tunnel. It shows the viewing hood, secondary lens, and two mirrors illustrated in Figure 15. The stop watch is located below the left mirror, out of view of the photograph.

Two 90 degree prisms are used to make the image splitter. The hypotenuse of one, after being coated with a half-silvered surface, is cemented to the hypotenuse of the other, forming a rectangular block. A much cleaner drop image is produced than with the simple half-silvered mirror used in the original set-up since ghost reflections from the non-silvered surface of the plane mirror are eliminated.

Figure 17 shows a schematic diagram of the switch box used for controlling the camera and selecting the subject to be photographed, i. e. the droplet or stop watch. Changing from one subject to the other is accomplished by merely switching from one illuminating source to the other while the camera is in operation. By photographing the droplet and stop watch at certain specified time intervals only, relatively few feet of film are required to record evaporating droplets having even the slowest evaporation rates. This allows the recording of several different droplets on one reel of film and makes it possible to record droplets whose total time of evaporation is greater than 2-1/2 minutes, the approximate duration of a 50 ft length of film at 16 frames per second.



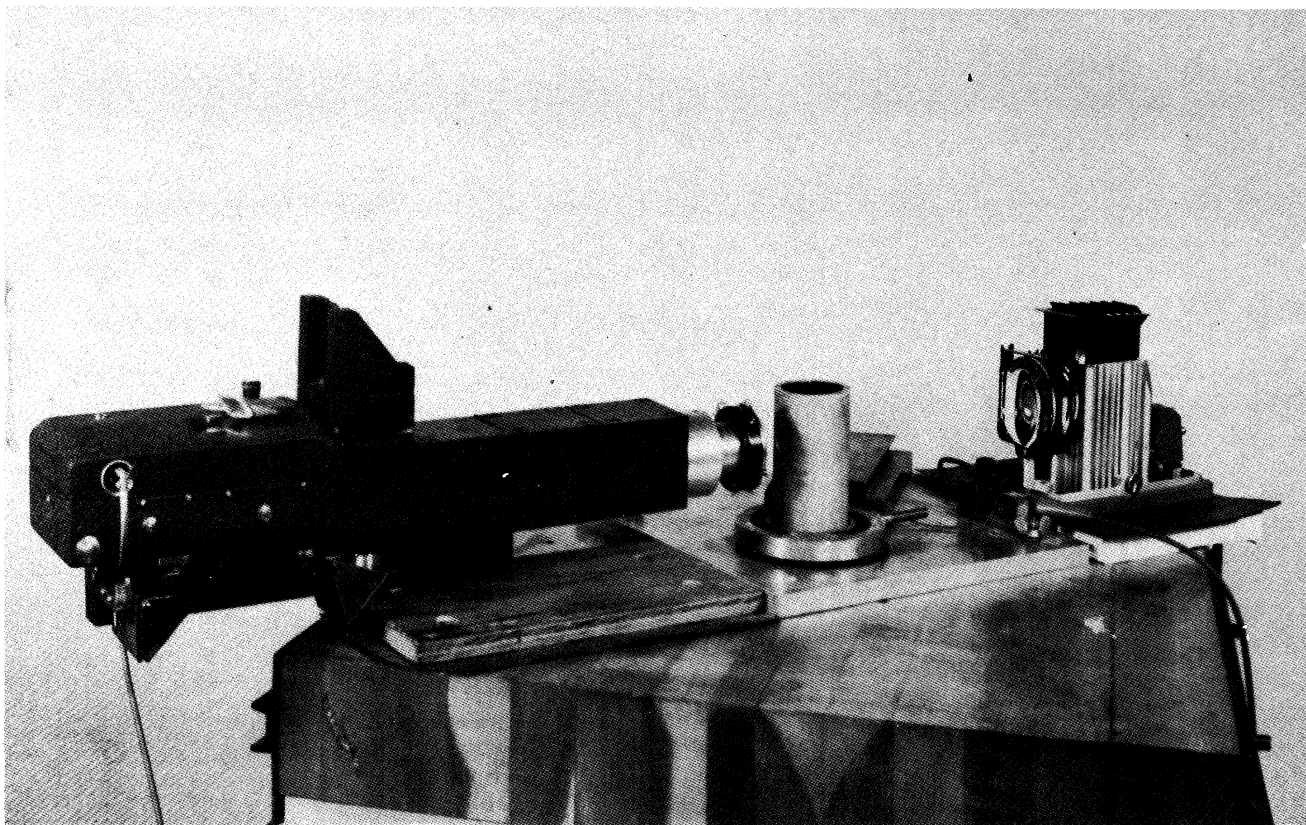


Fig. 16. Close-Up View of Camera, Barium Titanate Tube, and Droplet Light.

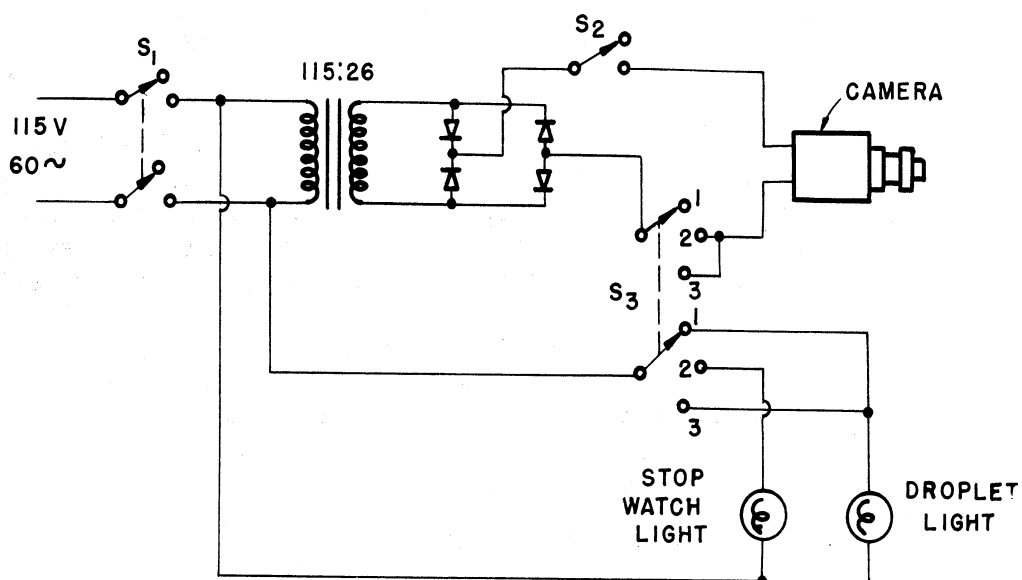


Fig. 17. Schematic of Switch Box.

## The Barium Titanate Piezoelectric Transducer

The stationary ultrasonic field is generated by a piezoelectric tube manufactured by the Brush Electronics Company. These tubes come in various sizes and shapes, and the particular units being used, and tested for possible use, in this application are shown in Figure 18. Only the large tubular element was used to obtain the results given in this report, but the smaller tubular units are being considered for the study of smaller droplets since theoretical considerations given in Appendix B indicate that the stabilizing effect of the ultrasonic field is proportional to the square of the frequency and inversely proportional to the drop diameter. The higher resonant frequencies of the smaller tubular elements should therefore provide a greater stabilizing action on the smaller droplets than has been obtained with the larger tube. In all tests performed with the large unit, the stabilizing effect on droplets disappeared at about 100 microns.

Dimensions of the large piezoelectric tube are  $1\frac{5}{8}$  O.D. x 2 I.D. x 4 inches long, and it operates at a resonant frequency of about 33,000 cps. Maximum safe operating voltage specified by the manufacturer is 100 volts rms, but most test runs were made at about 12 volts. The voltage is applied between the inner and outer coated surfaces of the tube.

Before the tube can be used for evaporation studies, it is necessary to fit the tube with two windows and then "tune" the tube by properly positioning these so as to cause the droplet to come to rest within the field of view of the windows.

Cutting and tuning are done in the following manner. A cutting tool is made from a one-half inch brass rod, about 2 inches long. The diameter of half the rod is reduced, if necessary, to fit the chuck of a vertical drill press, and the large end is drilled out with a three-eighths inch drill to a depth of about three-fourths inch, leaving a tubular wall thickness of one-sixteenth inch. The tool is completed by filing broad teeth in the tubular end.

Window positions are then laid out on diametrically opposite sides of the tube, about one-third of the distance from one end of the tube. One of these positions is surrounded by a small putty dam slightly less than one inch in diameter, and the tube is supported horizontally on the bed plate of the drill press by a half-round wooden rod slightly smaller than the inside diameter of the tube. After locating and lightly clamping the piezoelectric tube in position, the dam is partially filled with a diluted cutting compound. The cutting operation is carried out at a slow speed and with the drill handle weighted down to allow the operation to progress unattended. The cutting tool is lifted occasionally to allow the cutting compound to flow into the cut for better cutting and cooling.

When both holes are cut, half inch window discs, cut and ground to shape, are cemented in place. Before the cement hardens, however, the piezoelectric tube is mounted on the wind tunnel and connected to the output of the ultrasonic amplifier. A droplet of liquid is then suspended as described in EXPERIMENTAL PROCEDURE. If, after coming to rest, the droplet cannot be positioned between the two windows by varying the air velocity, it will be necessary to tune the unit. Three window adjustments are possible: a radial adjustment, a vertical angular adjustment, i.e. varying the angle between the window and the tube axis, and a horizontal angular adjustment, or varying the angle between the window and the tangent to the tube circumference. By varying the window positions and noting the effects on the drop position, it soon becomes possible to make the adjustments necessary to bring the droplet to rest between the two windows. The tube is then ready for use.

When an alternating voltage is impressed across the transducer, the tube changes shape as shown in Figure 19. One polarity causes the tube wall to thicken,

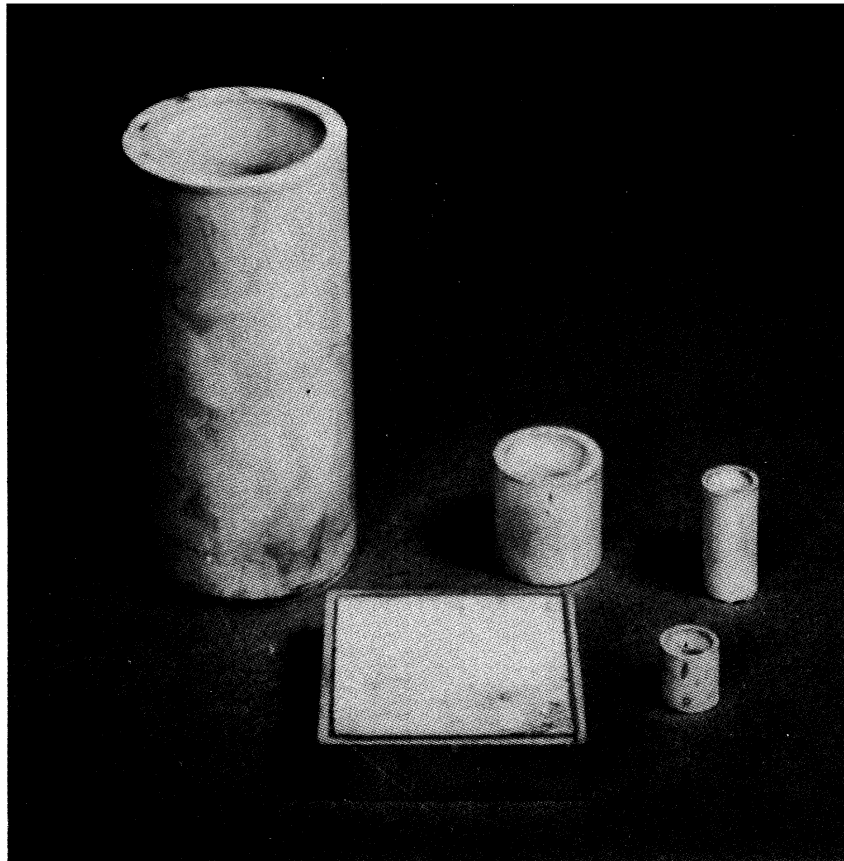


Fig. 18. Basic Piezoelectric Elements.

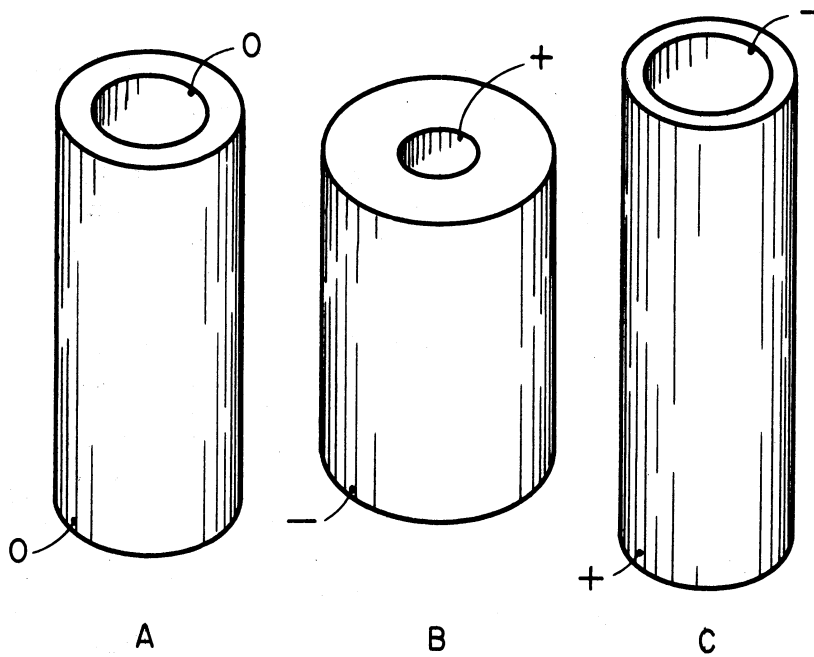


Fig. 19. Action of the Piezoelectric Tube Under Changes In Polarity of Applied Voltage.

Figure 19-B, thereby generating a radial compression wave within the tube, while the opposite polarity causes the tube wall to become thin, resulting in a radial rarefaction wave. Waves originating at a given position on the inner surface of the tube travel along a diameter to the opposite side of the tube; a similar wave travels in exactly the opposite direction at precisely the same time. When the tube diameter ( $d$ ) and wavelength ( $\lambda$ ) are properly related, ( $d = n\lambda$ ,  $n = 1, 2, \dots$ ) there results a stationary sound field as shown in Figure 20. The figure shows that two identical waves, traveling in opposite directions, combine to form a standing wave, i.e. a wave with stationary nodes. The droplet position in the field is indicated.

When using the large tube in a horizontal position, droplets of liquid of approximately 600 microns have been suspended against gravity solely by the action of the ultrasonic field. The droplets did exhibit some axial motion, possibly due to harmonics caused by the slightly distorted tube shape.

The condition required for a standing wave is that the tube diameter and wavelength have the relationship given above, i.e. the tube diameter be a whole multiple of the wavelength. A change in either the diameter or wavelength will upset the relationship and destroy the standing field. Since the tube diameter is fixed, only wavelength changes will affect the field, that is, either a change in frequency or velocity of the wave in air. Since the tube must operate within a very narrow frequency band around the resonant frequency, the field is essentially controlled by the sonic velocity in air. From the well known relationship for sonic velocity,

$$a = \sqrt{\gamma RT} = 49.1 \sqrt{T}$$

where

$$\begin{aligned} a &= \text{sonic velocity in ft/sec} \\ \gamma &= \text{ratio of specific heats } C_p/C_v = 1.4 \text{ for air} \\ R &= \text{gas constant} = 1715 \text{ ft-lb/slug } ^\circ\text{R} \\ T &= \text{degrees Rankine,} \end{aligned}$$

the fact is established that the ultrasonic field is dependent upon air temperature only and that any change in temperature will destroy the stationary field and, therefore, the stabilizing action on the droplet.

However, the possibility remains that the temperature can be changed by an amount such that the required relationship between wavelength and tube diameter be re-established. This has been done in Appendix C which shows that the required temperature changes are large and that at most, only two points are possible within what might be classed as a reasonable temperature range. The tube, therefore, is not adaptable to studies involving changes in temperature.

To overcome this effect, attention has been directed to the possibility of maintaining the proper wavelength - diameter (distance) relationship by changing the distance between the wave generating surfaces as the wavelength changes. Although impossible with the tube, this might be accomplished with flat parallel plates. Using four plates to form a square duct, it may be possible to create a standing field in which the stationary nodes form a square grid. Changing the distance between opposite plates by the proper amount would thus compensate for changes in wavelength due to changes in temperature, thereby maintaining the required wavelength - distance relationship and also the stabilizing effect on the droplet.

During the evaporation runs it was noted that as the droplets decreased in size the stability of the droplets decreased and finally disappeared when the

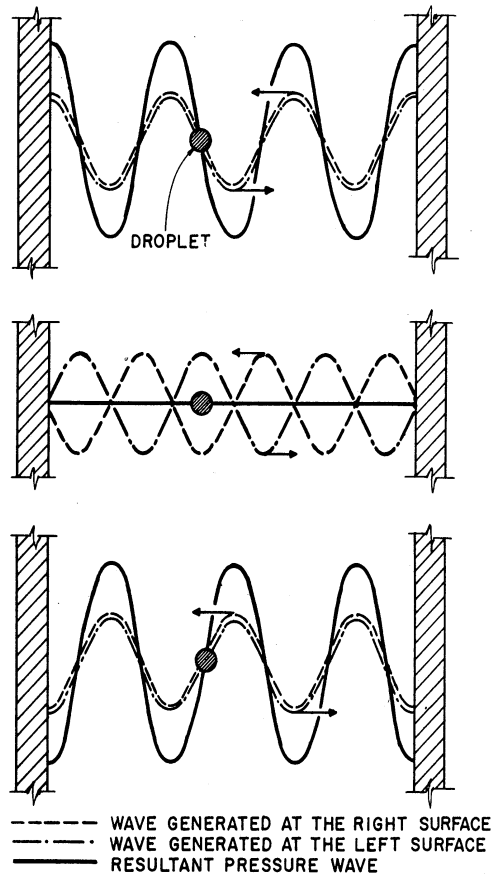


Fig. 20. Generation of the Standing Sound Wave by the Piezoelectric Tube.

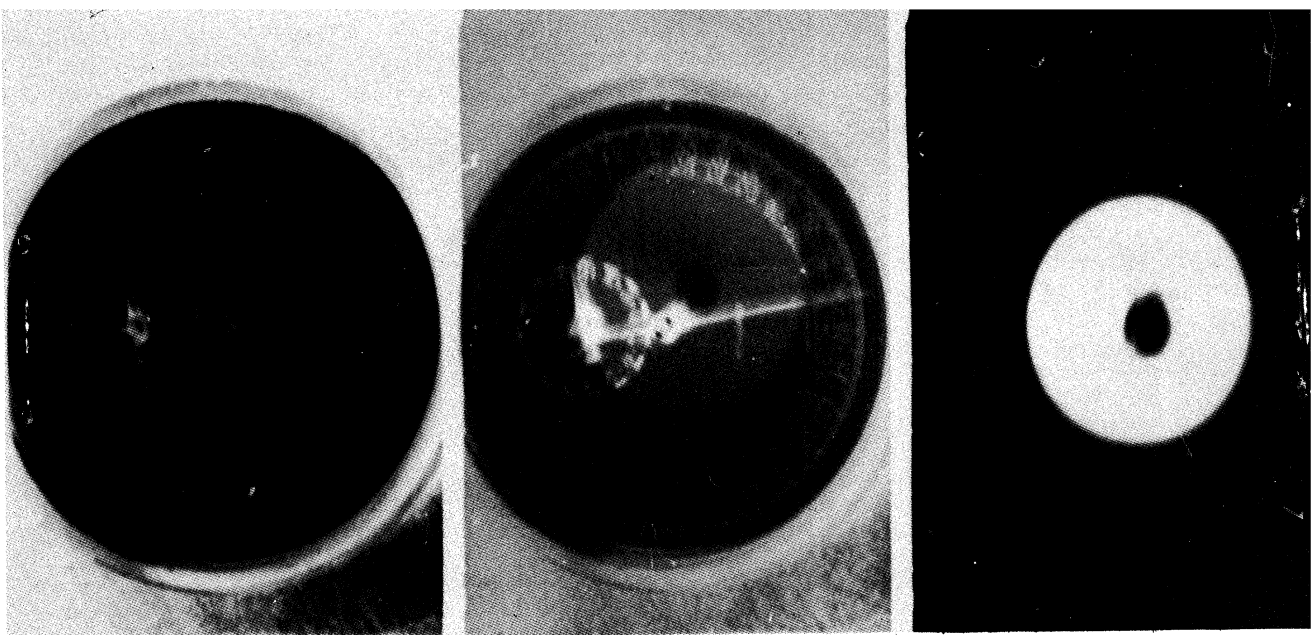


Fig. 21. Section of 16-mm Film Showing Change from Stop-Watch to Droplet Image.

diameter decreased to about 100 microns. This follows from the result derived in Appendix B which shows that the maximum droplet displacement is inversely proportional to the droplet diameter. It can be assumed, therefore, that when the displacement increases to a sufficient portion of the wavelength the stabilizing effect is permanently lost, and the droplet wanders about within the tube. The equation also shows the displacement to be inversely proportional to the square of the frequency, indicating that an increase in frequency should result in greater stability, so that tests with droplets smaller than 100 microns seem feasible. The flat plate element shown in Figure 18 operates at a resonant frequency of 200,000 cps, a considerable increase over the 33KC operating frequency of the tube being used at present. This indicates that evaporation studies can be extended to much smaller drop sizes than are possible with the present apparatus.

Work is in progress to adapt the flat plate elements to the present investigation in order to overcome the temperature effects mentioned earlier and to investigate droplets below 100 microns.

### Experimental Procedure

Before the equipment is used, the field of view of the camera should be marked on the viewing screen. A focusing screen is first made from a discarded film magazine and a piece of fine-grained ground glass and is inserted into the film magazine compartment. By focusing on a stationary flat object and noting the limits of the image appearing on the focusing screen, it becomes possible to mask the same image on the viewing screen with transparent scotch tape. A straight piece of fine wire glued to the end of a very fine thread is also required for focusing and size determination, as explained later.

The equipment, set up and connected as shown in Figures 11 and 12, is ready for its initial run. Several minutes before the run is to be made, the ultrasonic amplifier, oscillator, and variable D.C. supply are turned on and allowed to warm up. During this time the camera lens is opened, set to about  $f/4.5$ , and the focusing screen is inserted into the film magazine compartment. The power to the switch box is turned on and the control switch,  $S_3$  in Figure 17, set to position 1. This turns on the background light for the droplet. The lamp is positioned to give the best field of illumination when viewed on the viewing screen in the lens extension tube.

With the air turned on at a relatively low velocity and the ultrasonic supply warmed up, the oscillator is tuned to the resonant frequency of the tube (approximately 33,000 cps for the large tubular element). The voltage across the tube is then adjusted to about 20 volts by varying the D.C. supply. The wire is then suspended in the tube, close to the position originally occupied by the droplet during the window tuning operation. At the same time the oscillator frequency is varied until the wire is suddenly "grasped" by the sound field and held in a fixed position. The voltage is again adjusted to about 20 - 30 volts and a fine frequency adjustment is made to increase the "grasp" if possible. When the adjustment is correct, it is possible to slightly shift the upper end of the thread holding the wire without causing the wire to shift.

A glass eye-dropper, drawn to a fine tip, is next filled with a liquid of relatively low volatility, such as kerosene, and droplets are shaken from the dropper into the tube directly above the node previously occupied by the wire in the frequency adjustment operation. If the majority of the droplets fall, the air velocity should be increased. If they rise, the air velocity should be decreased. It will be found that eventually some droplets will be held suspended in the air stream. The air velocity should then be adjusted until the droplet occupies a



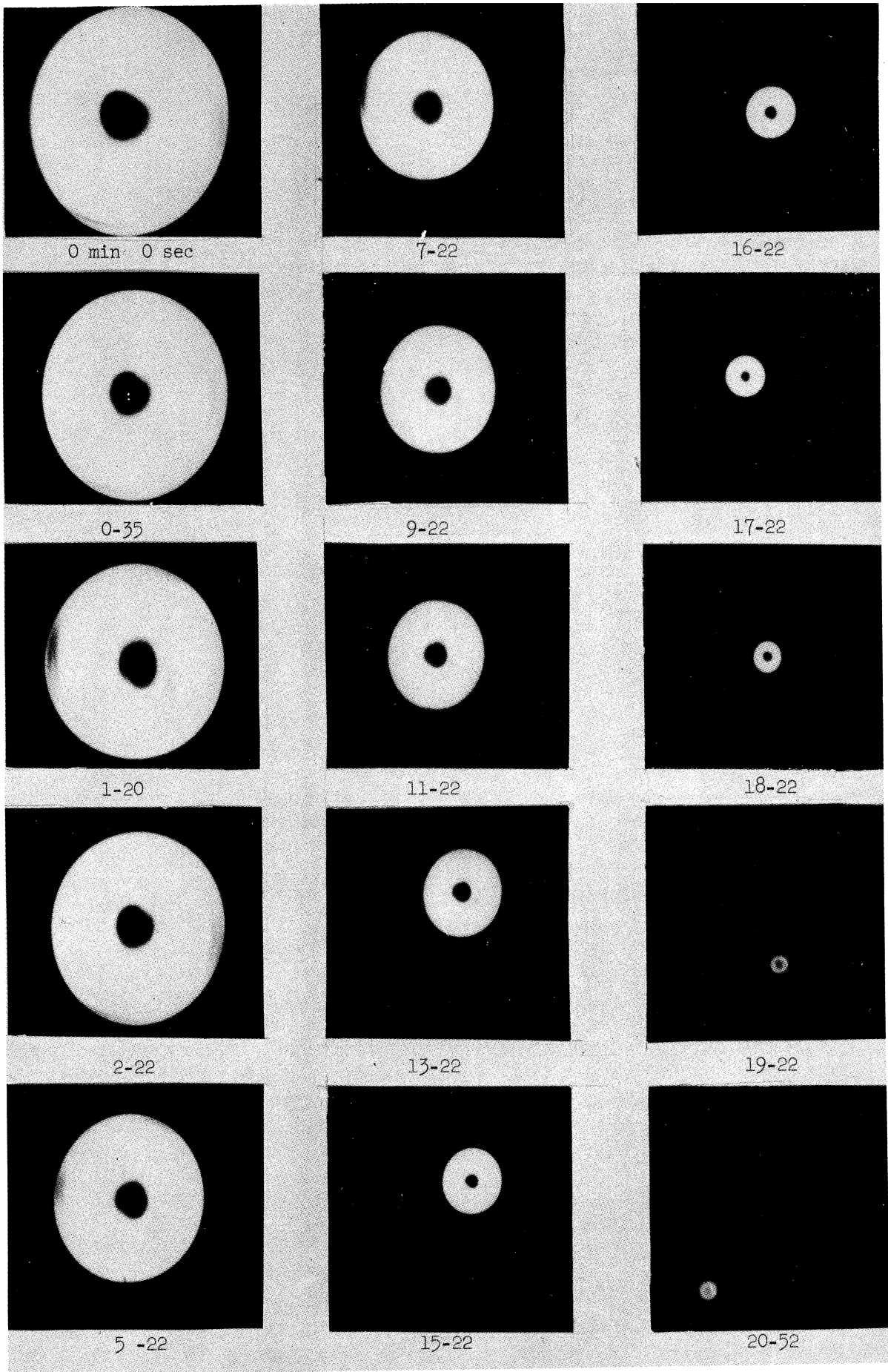


Fig. 22. Sequence of Frames Taken from a Film of an Evaporating Droplet (Acetophenone)-Elapsed Time Given in Minutes and Seconds.

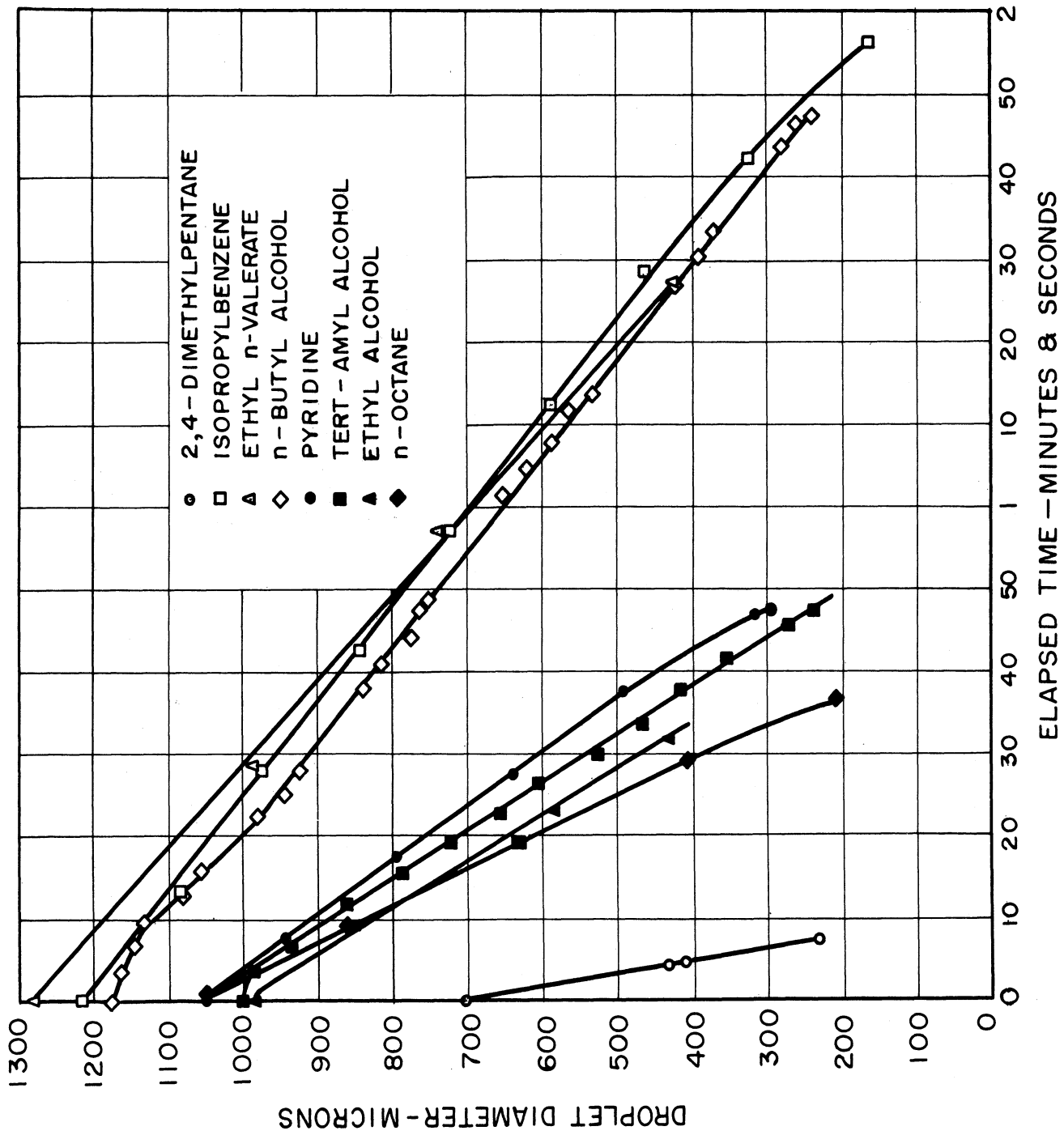


Fig. 23. Evaporation Curves for Some Pure Hydrocarbons, Diameter vs Elapsed Time.



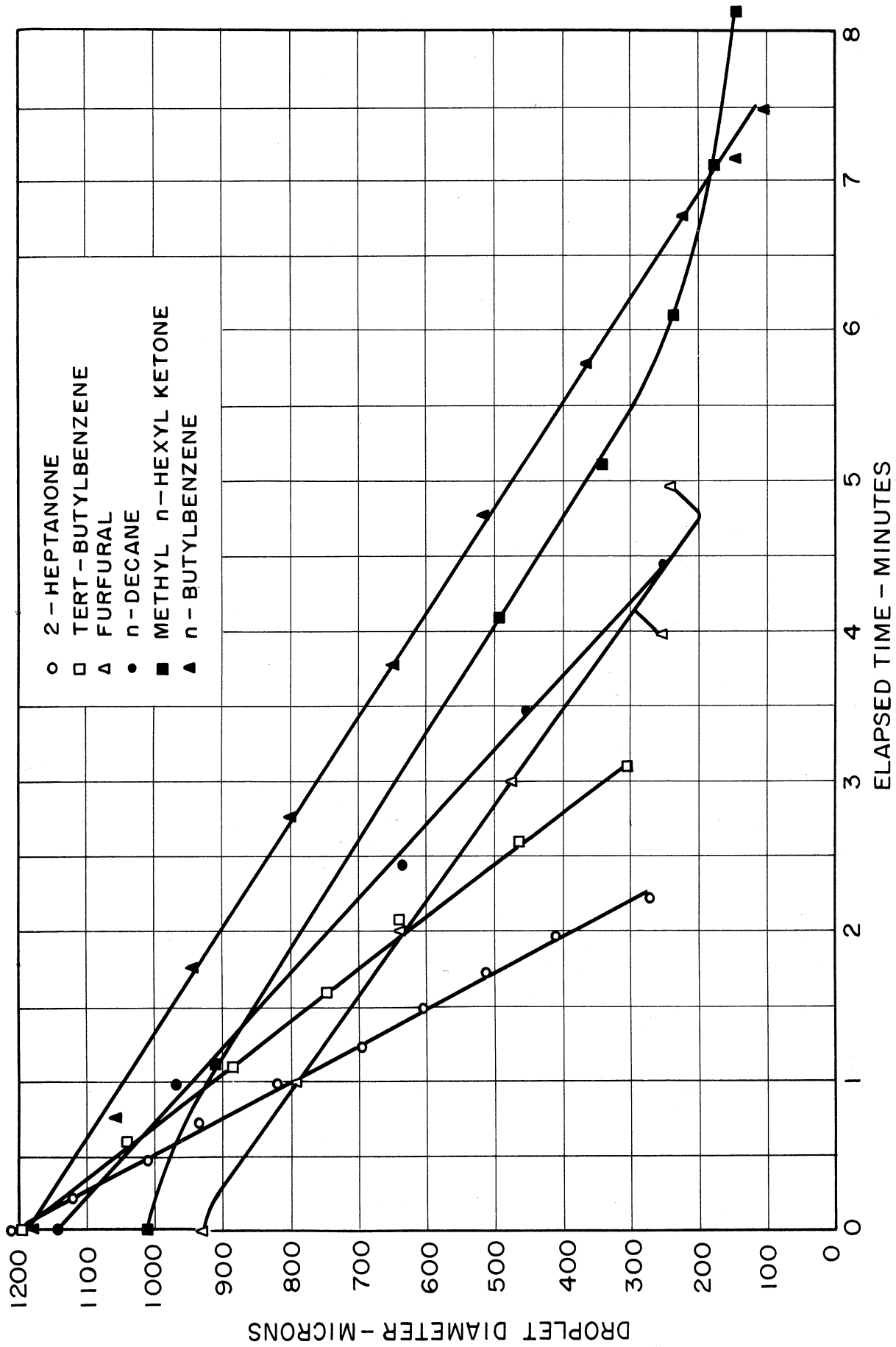


Fig. 24. Evaporation Curves for Some Pure Hydrocarbons, Diameter vs Elapsed Time.

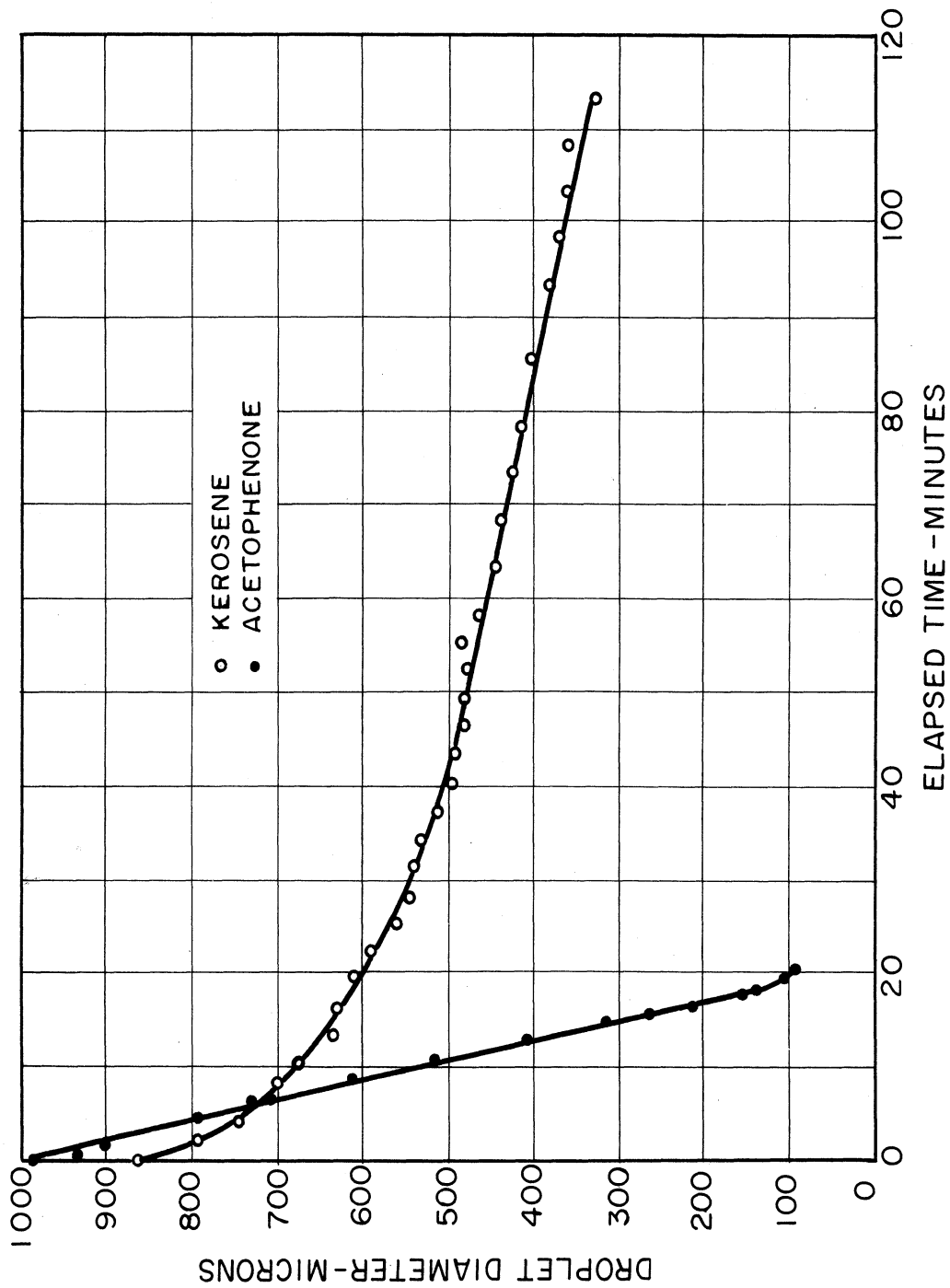


Fig. 25. Evaporation Curves, Diameter vs Elapsed Time.

position directly between the two windows and becomes visible on both the focusing and viewing screens. Using a pencil type microscope, about 20X, to view the image on the focusing screen, the camera is adjusted to bring the image into sharp focus.

The control switch  $S_3$  on the switch box is then turned to position 2 with switch  $S_2$  in the off position, turning on the stop watch light source and turning off the droplet light. The stop watch is then taped to a movable platform directly below the camera and in full view of the secondary lens as indicated in Figure 15. The light source is adjusted to get maximum illumination, and then the stop watch is brought into sharp focus by raising or lowering the platform.

When making a run, the equipment is allowed to warm up for about half an hour. During this time the eye-dropper is thoroughly cleaned and filled with the fuel to be checked. If the equipment has not been used for some time it may be necessary to retune the oscillator and to focus the camera. After selecting the correct lens opening and shutter speed, and setting the footage indicator, a "shot" is taken of the test number and another of the wire suspended in the ultrasonic field. By measuring the actual size of the wire and the size of the image on the developed film, a magnification factor is obtained. Droplets are then shaken into the cylinder until one becomes suspended, and a photographic record is immediately started. This is done with both switches  $S_1$  and  $S_2$ , see Figure 17, in the "on" position and the control switch  $S_1$  started in position 1. A shot is taken by turning the control switch to positions 2,3,2, and 1 in the given order. In position 2 the camera is turned on and the stop watch illuminated, thereby recording the time. In position 3 the camera is kept running while only the droplet is illuminated so that the droplet image is recorded. In going to positions 2 and 1 again, the time is recorded a second time, and the final position stops the camera and illuminates only the droplet so that its position can be controlled by manually varying the air flow. Shots are taken at about one-half or one minute intervals until it is no longer possible to control the drop position. Figure 21 shows the conversion from stop watch to droplet image during a typical shot.

The developed film is then projected on a screen to get an additional magnification. Here the wire image is accurately measured to obtain the overall magnification factor. The sharpest image from each shot of a droplet is then measured in two directions at right angles to each other to get average droplet diameter, and the time is computed from the closest stop watch image. The result gives average droplet diameter vs elapsed time of evaporation.

### Experimental Results

The experimental data were obtained with the large tubular element shown in Figure 17, and all tests were carried out at room temperature and pressure. In all cases the droplet was falling at its terminal velocity, a characteristic feature of the technique used. A typical film record is shown in Figure 22. All results are plotted in Figures 23, 24, and 25 and are summarized in Table III where the negative inverse slopes of the evaporation curves, in seconds/micron, are given for each pure hydrocarbon tested. The table also gives the boiling points and latent heats of vaporization, and these are plotted against the negative inverse slope in Figure 26.

The results show a linear relationship between droplet diameter and elapsed time of evaporation for the pure hydrocarbons. Slight deviations, however, from this linear relationship are noted at the start and finish of some of the runs. It is presently believed that these effects can be attributed to one or more of the following factors:

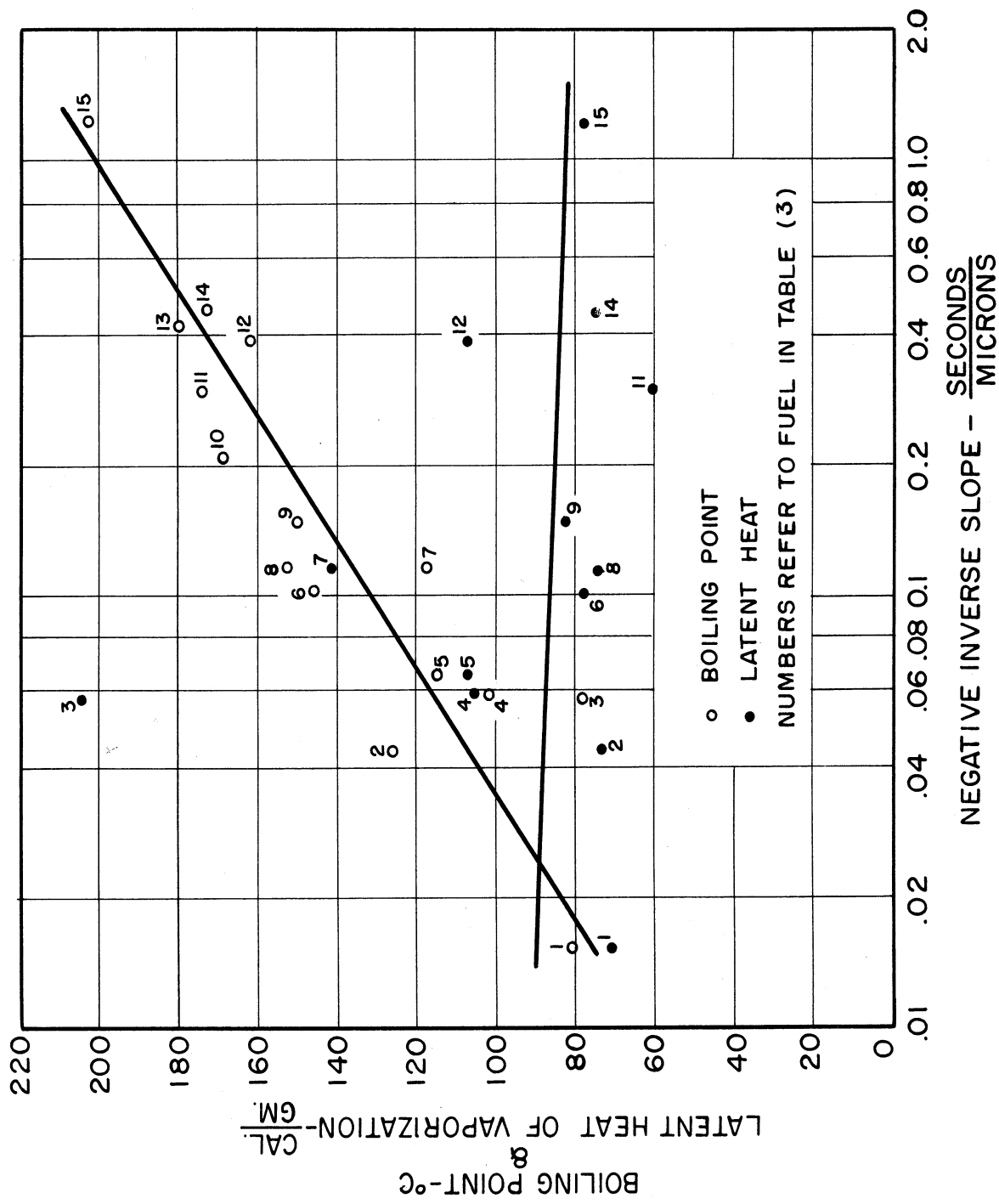


Fig. 26. Boiling Point and Latent Heat of Vaporization as a Function of Evaporation Rate for Some Pure Hydrocarbons.

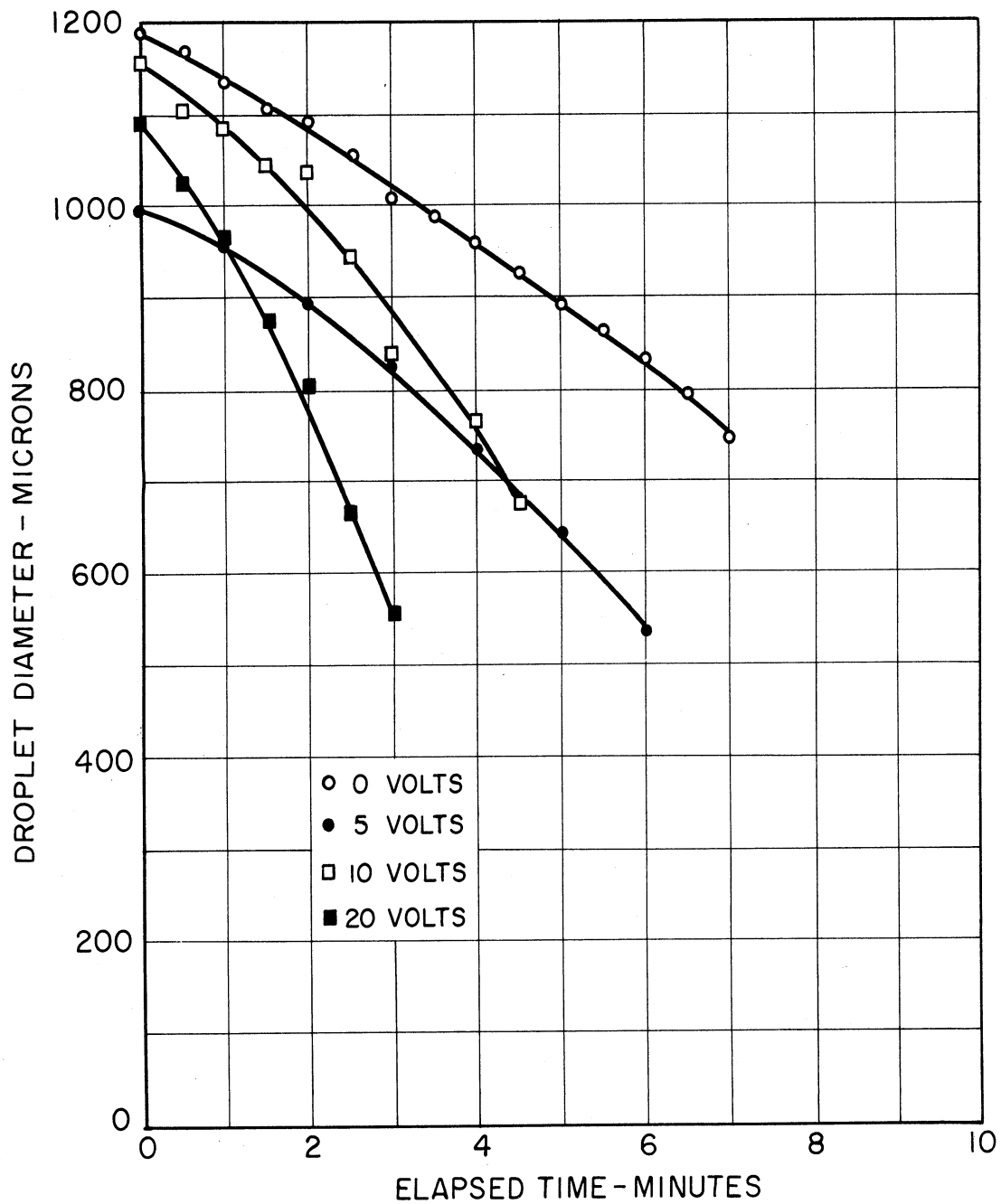


Fig. 27. Effect of Ultrasonic Field Intensity on Evaporation Rates (Tert-Butylbenzene)

- a. Initial cooling of the droplet upon entering the air stream.
- b. Impurities present in the fuels. The purity of the fuels tested ranged from 99 mol % to unspecified values. For the present developmental stages of the technique and apparatus this is considered adequate, but these will have to be replaced eventually with fuels of a uniform high purity.
- c. Changes in intensity of the ultrasonic field. During some of the runs, the intensity of the field was increased towards the end of the evaporation run to improve droplet stability. In view of recent tests discussed in a later section, the increased evaporation rate with an increased field intensity should be expected.

Figure 25 indicates that the evaporation process is influenced to a greater degree by the boiling point than by the latent heat since, in general, the rate increases with an increase in boiling point while the latent heat remains about constant. This is indicated by the solid lines drawn through the widely dispersed points. These lines are meant to show only the general trend of each property with rate of evaporation.

#### Effect of the Ultrasonic Field on Evaporation

Tests to investigate the effects of the ultrasonic field on evaporation have been initiated only a short time ago, so the results at this time are meager and inconclusive to some extent. However, it has been determined that some influence exists and that the effect increases with the intensity of the field, becoming quite pronounced at the higher intensities.

Some results are shown in Figure 27, indicating the increase in evaporation rate with increasing sound intensity. Tests were made in still air with droplets suspended in the sound field on a fine glass filament. At zero and 5 volts across the piezoelectric tube, the filament was clamped firmly to a support, while at the higher voltages the glass filament was suspended from a fine thread, allowing the droplet to find its equilibrium position in the sound field. The fuel used was tert-butylbenzene. The test carried out at zero volts represents, essentially, the technique used by Godsave, except that no burning took place.

An interesting factor to note is that the character of the evaporation curve changes when the evaporation takes place in still air, for under this condition the curves are no longer linear, as was true for all other tests in this investigation, but exhibit a definite curvature.

It is felt that additional tests will have to be made before definite conclusions can be reached on the ultrasonic effects. The results given are based on a single test run, and whether or not they can be repeated is not known. Additional work along these lines is being pursued.

TABLE III

## Evaporation Rates of Some Hydrocarbon Fuels

Fuel	Negative Inverse Slope ( $\frac{\text{Seconds}}{\text{Micron}}$ )	Boiling Point (°C)	Heat of Vaporization $\Delta H_v$ ( $\frac{\text{Calories}}{\text{Gram}}$ )
1 2,4-Dimethylpentane	0.015	80.8	70.9
2 n-Octane	0.044	125.7	73.19
3 Ethyl Alcohol	0.057	78.5	204.0
4 Tert-Amyl Alcohol	0.059	102.0	105.83
5 Pyridine	0.066	115.0	107.36
6 Ethyl n-Valerate	0.101	145.5	77.16
7 n-Butyl Alcohol	0.117	117.7	141.26
8 Isopropylbenzene	0.117	152.5	74.6
9 2-Heptanone	0.148	150.0	82.66
10 Tert-Butylbenzene	0.208	168.7	--
11 n-Decane	0.295	174.0	60.2
12 Furfural	0.385	161.7	107.51
13 n-Butylbenzene	0.418	180.0	--
14 Methyl n-Hexyl Ketone	0.454	173.0	74.06
15 Acetophenone	1.237	202.3	77.16

## BIBLIOGRAPHY

1. Bolt, J. A., Boyle, T. A., Mirsky, W., "The Generation and Burning of Uniform-Size Liquid Fuel Drops," Project 1988, University of Michigan Engineering Research Institute Report, May, 1953.
2. Godsave, G. A. E., "The Burning of Single Drops of Fuel," National Gas Turbine Establishment, England, Report R87, 1951.
3. Gohbrandt, W. "Evaporation of Spheres in a Hot Air Stream," National Gas Turbine Establishment, England, Memo No. M110, 1951.
4. Kinzer, G. D., and Gunn, R., "The Evaporation, Temperature and Thermal Relaxation - Time of Freely Falling Waterdrops," Journal of Meteorology, April, 1951.
5. Namekawa and Takahashi, "Note on the Evaporation of Small Water Drops," Physico-Mathematical Society of Japan, 1932.
6. Spalding, D. B., "Combustion of Liquid Fuel in a Gas Stream," Fuel, 29, 2-7 and 25-32 (1950).
7. Spalding, D. B., "Combustion of Fuel Particles," Fuel, 30, 121-130 (1951).
8. Topps, J. E. C., "An Experimental Study of the Evaporation and Combustion of Falling Droplets," National Gas Turbine Establishment, Memorandum No. M105, February, 1951.





APPENDIX A

DATA FOR COMBUSTION OF BENZENE DROPS

Original Drop Size 80 Microns

Picture No.	Zone										
	1	2	3	4	5	6	7	8	9	10	11
1128	80 70 <sup>2</sup>	80 <sup>2</sup> 70	70 <sup>2</sup> 60	80 70 60	70 <sup>2</sup> 60	70 60 <sup>2</sup>	70 <sup>2</sup> 60	60 <sup>2</sup> 50	50 <sup>2</sup> 40	70 50 <sup>2</sup>	
1153	80	80	70	70	60	60	60	60		40	
1154	80 <sup>3</sup> 70 <sup>3</sup>	80 <sup>2</sup> 70 <sup>4</sup>	80 70 <sup>4</sup> 60	80 70 <sup>4</sup> 60	80 <sup>2</sup> 70 <sup>2</sup> 60 <sup>2</sup>	70 <sup>3</sup> 60 <sup>2</sup>	60 <sup>4</sup> 50				
1155	80	70	80	70	60	70	60				
1172	80 <sup>5</sup> 70	80 <sup>4</sup> 70 <sup>4</sup>	80 <sup>5</sup> 70 <sup>13</sup> 60	80 <sup>2</sup> 70 <sup>13</sup> 60 <sup>5</sup>	80 70 <sup>8</sup> 60 <sup>6</sup>	70 <sup>2</sup> 60 <sup>7</sup> 50	60 <sup>5</sup> 50 <sup>2</sup> 40				

Mean Drop Diameter - Microns

76.0	74.5	71.4	69.0	66.8	61.4	57.2	57.5	46.7	52.5
------	------	------	------	------	------	------	------	------	------

Mean Velocity - Fr/Sec

6.85	5.12	5.4	5.02	4.91	4.75	4.20	6.42	1.43	1.59
------	------	-----	------	------	------	------	------	------	------

Mean Time to Traverse Width fo Zone - Seconds x 10<sup>2</sup>

.101	.134	.131	.138	.141	.146	.165	.108	.514	.436
------	------	------	------	------	------	------	------	------	------

Elapsed Time - Seconds x 10<sup>2</sup>

0	.101	.235	.366	.504	.645	.791	.956	1.064	1.578
---	------	------	------	------	------	------	------	-------	-------

1. Values tabulated are drop diameters in microns
2. Superscript indicates numbers of given size appearing in zone

DATA FOR COMBUSTION OF n-HEPTANE DROPS

Picture No.	Zone											
	1	2	3	4	5	6	7	8	9	10	11	
1211	110	100 <sup>2</sup>	90	90	100	90 <sup>4</sup>	90 <sup>2</sup>	80				
	100			80	80			70				
1223	100	110	110	110 <sup>2</sup>	90	90	80 <sup>2</sup>	80 <sup>2</sup>	90	70	50	
	90	100	100	100	80				80			
1227	110	110 <sup>2</sup>	90	90 <sup>2</sup>	90	90 <sup>2</sup>	90	90	60			
		100	100 <sup>2</sup>	100 <sup>3</sup>					70			70
1228	100			90		90 <sup>2</sup>	90	90				40 <sup>3</sup>
1229	100	100	110	100	110 <sup>2</sup>	80	90	80	80			
				80 <sup>3</sup>	90 <sup>3</sup>	70	80					
1233			90	80	80	70	80	40				
1234	110	90	90	90 <sup>2</sup>	70	80	80	80	70			
1236	100	100	100	100	100	90 <sup>3</sup>	80	50	50			
	110			80	90	80 <sup>2</sup>	50		40			
1245	100 <sup>3</sup>	100 <sup>2</sup>		100	90	100	90 <sup>2</sup>	80	70 <sup>2</sup>			
					80	90 <sup>3</sup>	70		50			
1247				100	90 <sup>2</sup>	90	80 <sup>2</sup>		70			
				90	80 <sup>2</sup>	80 <sup>5</sup>	70 <sup>2</sup>					
				80	70 <sup>2</sup>	70 <sup>2</sup>	60					

Mean Drop Diameter - Microns

102 102 98 92 87.3 87.8 81 75 69 70 50

Mean Drop Velocity - Ft/Sec

6.25 5.33 4.85 4.65 3.85 3.24 3.74 3.02 1.40 4.57 1.51

Mean Time to Traverse Zone - Seconds x 10<sup>2</sup>

.111 .130 .143 .149 .180 .214 .185 .229 .495 .155 .457

Elapsed Time - Seconds x 10<sup>2</sup>

0 .111 .241 .384 .533 .713 .927 1.112 1.34 1.84 1.99

DATA FOR COMBUSTION OF PROPANOL DROPS

Picture No.	Zone										
	1	2	3	4	5	6	7	8	9	10	11
1532	80 <sup>4</sup>	80 <sup>4</sup>	80 <sup>2</sup>	80	80	70 <sup>3</sup>	60 <sup>3</sup>	60 <sup>2</sup>	50		
			70 <sup>2</sup>	70 <sup>3</sup>	70 <sup>3</sup>	60	30	50	40 <sup>3</sup>		
1533	80 <sup>6</sup>	80 <sup>6</sup>	80 <sup>6</sup>	70 <sup>6</sup>	70 <sup>5</sup>	70 <sup>3</sup>	60 <sup>3</sup>	60 <sup>2</sup>	60 <sup>4</sup>		
					60	60 <sup>3</sup>	50 <sup>3</sup>	50 <sup>3</sup>	50 <sup>2</sup>		
1536	80 <sup>5</sup>	80 <sup>4</sup>	80 <sup>5</sup>	70	70 <sup>2</sup>	60 <sup>3</sup>	60 <sup>2</sup>	60	50 <sup>2</sup>		
		50	80	60 <sup>2</sup>	60 <sup>3</sup>	50 <sup>2</sup>	50 <sup>2</sup>	60	40		
			70	50 <sup>2</sup>			40	40	30		
			60 <sup>2</sup>					30			
			50								
1526	80 <sup>2</sup>	80 <sup>2</sup>	60	70	70	70	60				
		70									
1518	80 <sup>4</sup>	80 <sup>3</sup>	80 <sup>2</sup>	80	70 <sup>3</sup>	70	60 <sup>2</sup>				
			70 <sup>2</sup>	70		50	40				
1519	80 <sup>9</sup>	80 <sup>7</sup>	80	80	70 <sup>3</sup>	60 <sup>3</sup>	70				
			70 <sup>3</sup>	70 <sup>4</sup>	60 <sup>3</sup>	50 <sup>3</sup>	60 <sup>5</sup>				
			60	60			50 <sup>2</sup>				
1506	80 <sup>3</sup>	80 <sup>2</sup>	80	50	60 <sup>2</sup>						
			70 <sup>2</sup>	70 <sup>2</sup>							
1492	80 <sup>6</sup>	80 <sup>2</sup>	80 <sup>2</sup>	80 <sup>2</sup>	70 <sup>6</sup>						
			70 <sup>7</sup>	70	60 <sup>2</sup>						
			60 <sup>2</sup>	60 <sup>2</sup>							
Mean Drop Diameter - Microns	80	78.7	74.9	69.2	66.5	61.2	53.8	51.4	49.3		
Mean Velocity - Ft/Sec	6.74	5.59	4.95	4.38	3.78	3.43	1.72	.736	1.22		
Mean Time to Traverse Zone - Seconds x 10 <sup>2</sup>	.103	.124	.140	.158	.183	.202	.404	.943	.565		
Elapsed Time - Seconds x 10 <sup>2</sup>	0	.103	.227	.367	.525	.708	.910	1.314	2.257		

DATA FOR COMBUSTION OF CYCLOHEXANE DROPS

Picture No.	Zone													
	1	2	3	4	5	6	7	8	9	10	11	12	13	14
1263	110 <sup>2</sup>	100 <sup>3</sup>	90 <sup>4</sup>	90 <sup>3</sup>	100	80 <sup>3</sup>	80	70 <sup>3</sup>	60 <sup>2</sup>	70 <sup>2</sup>	70	50	50 <sup>2</sup>	60 <sup>2</sup>
	100 <sup>2</sup>	90	80	80	90	70	70 <sup>3</sup>	60		40	40		40	30
1264	100 <sup>2</sup>	100	100 <sup>2</sup>	90 <sup>2</sup>	80 <sup>2</sup>	80 <sup>2</sup>	80	40	90 <sup>2</sup>	80	80	90	70	
		90							70	60	50	60	60	
1266	100 <sup>2</sup>	100 <sup>2</sup>	90 <sup>2</sup>	90 <sup>2</sup>	90 <sup>2</sup>	80	80	90	80	80	80			
1305	100 <sup>2</sup>	100 <sup>2</sup>	100	90	80	70	70	70	80	70	50			
			90	90	80	60	60	70	80	80	70 <sup>2</sup>			
1307	100	100 <sup>4</sup>	100 <sup>3</sup>	100 <sup>2</sup>	100	90 <sup>7</sup>	90 <sup>4</sup>	90 <sup>2</sup>	70	60	60			
			90 <sup>5</sup>	90 <sup>9</sup>	90 <sup>15</sup>	80 <sup>11</sup>	80 <sup>4</sup>	80 <sup>2</sup>	60 <sup>2</sup>	60 <sup>2</sup>				
			80 <sup>2</sup>	80 <sup>6</sup>	80 <sup>4</sup>	70	70 <sup>2</sup>	70 <sup>2</sup>						
				70	70	60	60	60						
Mean Drop Diameter - Microns	102	98.5	92.3	88.1	87.5	80.4	76.2	71.4	69.0	63.2	62.0	53.4	51.6	50.0
Mean Drop Velocity - Ft/Sec	8.5	7.51	6.08	6.03	6.19	5.58	4.20	4.38	3.48	2.84	2.31	2.72	3.37	2.04
Mean Time to Traverse Width or Zone - Sec x 10 <sup>2</sup>	.0825	.092	.114	.115	.112	.124	.165	.158	.199	.244	.288	.255	.206	.340
Elapsed Time - Seconds x 10 <sup>2</sup>	0	.0825	.1745	.2885	.4035	.527	.692	.850	1.049	1.293	1.537	1.825	2.080	2.286



APPENDIX B



## APPENDIX B

### Development of the Equation for the Stabilizing Action of the Ultrasonic Field on Drop Position

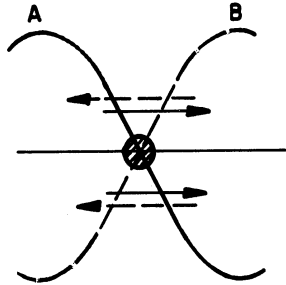


Fig. A.

Figure A illustrates the position of a droplet in the node of a standing sound wave. At a given instant, let the pressure distribution be represented by the solid curve A. Under these conditions, air will flow past the droplet from left to right as designated by the solid arrows. Half a period later, the pressure can be represented by the dotted curve B and the air velocity by the dotted arrows from right to left. The air velocity relative to the drop can then be represented by the following equation:

$$V = V_m \sin \omega t. \quad (1)$$

where

$$\begin{aligned} V &= \text{relative velocity at time } t \\ V_m &= \text{maximum relative velocity} \\ \omega &= \text{frequency of the ultrasonic sound} \\ t &= \text{time} \end{aligned}$$

This relative velocity gives rise to a drag force on the drop, where the drag force is related to a drag coefficient by the following expression.

$$C_D = \frac{D}{(1/2)\rho_a V^2 S} \quad (2)$$

where

$$\begin{aligned} C_D &= \text{drag coefficient (dimensionless)} \\ D &= \text{drag force (pounds)} \\ \rho_a &= \text{mass density of air (slug/ft}^3\text{)} \\ V^a &= \text{relative velocity of the air} \\ &\quad \text{past the drop (ft/sec)} \\ S &= \text{projected area of the drop (ft}^2\text{)} \end{aligned}$$

From this, the drag force is given by,

$$D = (1/2) \rho_a V^2 S C_D$$

Substituting for  $V$  from equation (1) we get the drag force as a function of time, i.e.,

$$D(t) = (1/2) \rho_a V_m^2 S C_D \sin^2 \omega t = D_M \sin^2 \omega t \quad (3)$$

where

$$\begin{aligned} D(t) &= \text{drag force as a function of time} \\ D_m &= \text{maximum drag force} \end{aligned}$$

Since the motion of the droplet is subject to Newton's equation of motion, the equation becomes

or  $\text{Drop mass} \times \text{acceleration} = \sum \text{forces causing the acceleration}$

$$M \frac{d^2x}{dt^2} = D_m \sin^2 \omega t \quad (4)$$

Integrating with respect to t,

$$\int \frac{d}{dt} \left( \frac{dx}{dt} \right) dt = \frac{D_m}{wM} \int \sin wt \, w dt \quad (5)$$

$$\frac{dx}{dt} = - \frac{D_m}{wM} \cos wt + C_1 \quad (6)$$

Here we substitute the initial condition:

$$\left\{ \begin{array}{l} t = 0 \\ \frac{dx}{dt} = v_0 \end{array} \right\} \quad (7)$$

so that

$$v_0 = - \frac{D_m}{wM} + C_1 \quad (8)$$

$$C_1 = v_0 + \frac{D_m}{wM} \quad (9)$$

Equation (6) becomes,

$$\frac{dx}{dt} = \left( v_0 + \frac{D_m}{wM} \right) - \frac{D_m}{wM} \cos wt \quad (10)$$

Integrating a second time with respect to t, we obtain,

$$\int \frac{d}{dt} (x) dt = \left( v_0 + \frac{D_m}{wM} \right) \int dt - \frac{D_m}{w^2 M} \int \cos wt \, w dt \quad (11)$$

which becomes,

$$x = \left( v_0 + \frac{D_m}{wM} \right) t - \frac{D_m}{w^2 M} \sin wt + C_2 \quad (12)$$

Substituting the initial condition:

$$\left\{ \begin{array}{l} t = 0 \\ x = 0 \end{array} \right\} \quad (13)$$

equation (12) becomes,

$$0 = C_2 \quad (13)$$

The general equation of motion is then given as,

$$\boxed{x = \left( v_0 + \frac{D_m}{wM} \right) t - \frac{D_m}{w^2 M} \sin wt} \quad (14)$$

Equation (14) shows that the displacement is made up of a continuously increasing term  $(v_0 + D_m/wM) t$  plus a sinusoidally varying term  $-(D_m/w^2M) \sin wt$ . Experimental results show, however, that x does not increase or decrease continuously with t. Since all the terms in the parentheses are constants, the following must be true to uphold the observed experimental result:

$$v_0 + \frac{D_m}{wM} = 0 \quad (t \geq 0) \quad (15)$$

so that

$$v_0 = - \frac{D_m}{wM} \quad (16)$$

The equation of motion for the droplet therefore reduces to

$$x = -\frac{D_m}{w^2 M} \sin wt \quad (17)$$

from which we obtain the maximum displacement

$$x_{\max} = -\frac{D_m}{w^2 M} \quad (18)$$

Substituting the following relations,

$$D_m = (1/2) \rho_a V_m^2 S C_D \quad (19)$$

$$M = (4/3) \pi r^3 \rho_l \quad (20)$$

$$S = \pi r^2 \quad (21)$$

and

$$w = 2\pi f \quad (22)$$

equation (18) becomes,

$$x_{\max} = -\frac{\frac{1}{2} \rho_a V_m^2 \pi r^2 C_D}{(2\pi f)^2 \left(\frac{4}{3}\right) \pi r^3 \rho_l}$$

$$x_{\max} = -\frac{3}{16\pi^2} \left(\frac{C_D}{d}\right) \left(\frac{\rho_a}{\rho_l}\right) \left(\frac{V_m}{f}\right)^2 \quad (24)$$

or

$$x_{\max} = 1.9 \times 10^{-2} \left(\frac{C_D}{d}\right) \left(\frac{\rho_a}{\rho_l}\right) \left(\frac{V_m}{f}\right)^2 \quad (25)$$

where

- x = droplet displacement (ft)
- C<sub>D</sub> = drag coefficient (dimensionless)
- d = drop diameter (ft)
- ρ<sub>a</sub> = mass density of the air (slugs/ft<sup>3</sup>)
- ρ<sub>l</sub> = mass density of the droplet (slugs/ft<sup>3</sup>)
- V<sub>m</sub> = maximum relative velocity of air and droplet (ft/sec)
- f = ultrasonic frequency (cps)

and

$$\left\{ \begin{array}{l} 1 \text{ ft} = 30.48 \times 10^4 \text{ micron} \\ \rho_a = 0.002378 \text{ slugs/ft}^3 \\ \rho_{\text{water}} = 1.94 \text{ slugs/ft}^3 \end{array} \right.$$

Assuming:

fixed droplet diameter (solid sphere) d = 500 microns  
V<sub>m</sub> = 500 ft/sec  
standard atmosphere

we get

$$\nu = \frac{\mu}{\rho} = \frac{3.719 \times 10^{-7}}{2.378 \times 10^{-3}} = 1.567 \times 10^{-4} \text{ ft}^2/\text{sec}$$

$$Re = \frac{dv}{\nu} = \left(\frac{500}{304.8 \times 10^3}\right) \frac{500}{1.567 \times 10^{-4}}$$

$$Re = 5230$$

For this value of Reynolds number, Goldstein gives the value of  $C_D = 0.4$  for solid spheres. Substituting in equation (25),

$$x_{\max} = 1.9 \times 10^{-2} \left( \frac{0.4}{500/304.8 \times 10^3} \right) \left( \frac{.002378}{1.94} \right) \left( \frac{500}{33,000} \right)^2$$

$$x_{\max} = 0.398 \text{ microns}$$

It must be remembered that this value is based on the following assumed conditions:

$$\begin{aligned} V_m &= 500 \text{ ft/sec} \\ C_D &= \text{constant} \end{aligned}$$

The result indicates that the maximum displacements of droplets in the node of an ultrasonic field are very small, an experimentally observed fact.



APPENDIX C



## APPENDIX C

## Temperatures at Which a Stationary Sound Field is Established in the Piezoelectric Tube

The sonic velocity is given by

$$a = \sqrt{\gamma RT}$$

where

$$\begin{aligned} \gamma &= 1.4 \\ R &= 1715 \\ T &= 460 + ^\circ\text{F} \end{aligned}$$

so that

$$a = 49.1 \sqrt{460 + ^\circ\text{F}} \text{ ft/sec}$$

For a given sound frequency, the wavelength,  $l$  is given by,

$$l = \frac{a}{f} = \frac{(49.1 \sqrt{460 + ^\circ\text{F}}) 12}{33,000} \text{ inches}$$

The number of wavelengths per tube diameter then becomes,

$$\begin{aligned} \frac{d}{l} &= \frac{1.625 (33,000)}{12(49.1) \sqrt{460 + ^\circ\text{F}}} \\ \frac{d}{l} &= \frac{91}{\sqrt{460 + ^\circ\text{F}}} \end{aligned}$$

For the indicated number of wavelengths, the required temperature becomes,

$$\begin{aligned} \frac{d}{l} = 2 & : \quad ^\circ\text{F} = \left(\frac{91}{2}\right)^2 - 460 = 1610^\circ\text{F} \\ \frac{d}{l} = 3 & : \quad ^\circ\text{F} = \left(\frac{91}{3}\right)^2 - 460 = 454^\circ\text{F} \\ \frac{d}{l} = 4 & : \quad ^\circ\text{F} = \left(\frac{91}{4}\right)^2 - 460 = 58^\circ\text{F} \end{aligned}$$

These results are based on an assumed resonant frequency of 33,000 cps. Actual resonance was established at 80°F, requiring a resonant frequency of 33,700 cps, while the manufacturers gives a general resonant frequency of 36,000 cps for this type of tube.